



HAL
open science

Isonitrile ruthenium and iron PNP complexes: synthesis, characterization and catalytic assessment for base-free dehydrogenative coupling of alcohols

Duc Hanh Nguyen, Delphine Merel, Nicolas Merle, Xavier Trivelli, Frédéric Capet, Régis Gauvin

► **To cite this version:**

Duc Hanh Nguyen, Delphine Merel, Nicolas Merle, Xavier Trivelli, Frédéric Capet, et al.. Isonitrile ruthenium and iron PNP complexes: synthesis, characterization and catalytic assessment for base-free dehydrogenative coupling of alcohols. Dalton Transactions, 2021, 50 (29), pp.10067-10081. 10.1039/d1dt01722e . hal-03358571

HAL Id: hal-03358571

<https://hal.science/hal-03358571v1>

Submitted on 29 Sep 2021

HAL is a multi-disciplinary open access archive for the deposit and dissemination of scientific research documents, whether they are published or not. The documents may come from teaching and research institutions in France or abroad, or from public or private research centers.

L'archive ouverte pluridisciplinaire **HAL**, est destinée au dépôt et à la diffusion de documents scientifiques de niveau recherche, publiés ou non, émanant des établissements d'enseignement et de recherche français ou étrangers, des laboratoires publics ou privés.

Isonitrile ruthenium and iron PNP complexes: Synthesis, characterization and catalytic assessment for base-free dehydrogenative coupling of alcohols.

Duc Hanh Nguyen,^a Delphine Merel,^a Nicolas Merle,^a Xavier Trivelli,^b Frédéric Capet^a and Régis M. Gauvin^{*,c}.

^a Univ. Lille, CNRS, Centrale Lille, ENSCL, Univ. Artois, UMR 8181 - UCCS - Unité de Catalyse et Chimie du Solide, F-59000 Lille, France

^b Université de Lille, CNRS, INRA, Centrale Lille Institute, Univ. Artois, FR 2638 - IMEC - Institut Michel-Eugène Chevreul, F-59000 Lille, France

^c Chimie ParisTech, PSL University, CNRS, Institut de Recherche de Chimie Paris, 75005 Paris, France.

E-mail : regis.gauvin@chimieparistech.psl.eu

ABSTRACT: Neutral and ionic ruthenium and iron aliphatic PNP-type pincer complexes (PNP= NH(CH₂CH₂PiPr₂)₂) bearing benzyl, *n*-butyl or *tert*-butyl isocyanide ancillary ligands have been prepared and characterized. Reaction of [RuCl₂(PNP)]₂ with one equivalent CN-R per ruthenium center affords complexes [RuCl₂(PNP)(CNR)] (R= benzyl, **1a**, R= *n*-butyl, **1b**, R= *t*-butyl, **1c**), with cationic [RuCl(PNP)(CNR)]₂Cl **2a-c** as side-products. Dichloride species **1a-c** react with excess NaBH₄ to afford [RuH(PNP)(BH₄)(CN-R)] **3a-c**, analogues to benchmark Takasago catalyst [RuH(PNP)(BH₄)(CO)]. Reaction of **1a-c** with a single equivalent of NaBH₄ results in formation of [RuHCl(PNP)(CN-R)] (**4a-c**), from which **3a-c** can be prepared upon reaction with excess NaBH₄. Use of one equivalent of NaHBET₃ with **4a** and **4c** affords bishydrides [Ru(H)₂(PNP)(CN-R)] **5a** and **5c**. Deprotonation of **4c** by KOtBu generates amido derivative [RuH(PNP)(CN-*t*-Bu)] (**6**, PNP= N(CH₂CH₂PiPr₂)₂), unstable in solution. Addition of excess benzyliisonitrile to **4a** provides cationic hydride [RuH(PNP)(CN-CH₂Ph)]₂Cl (**7**). Concerning iron chemistry, [Fe(PNP)Br₂] reacts with one equivalent of benzyliisonitrile to afford [FeBr(PNP)(CNCH₂Ph)]₂Br (**8**). The outer-sphere bromide anion can be exchanged by salt metathesis with NaBPh₄ to generate [FeBr(PNP)(CNCH₂Ph)]₂(BPh₄) (**9**). Cationic hydride species [FeH(PNP)(CN-*t*-Bu)]₂(BH₄) (**10**) is prepared from consecutive addition of excess CN-*t*-Bu and NaBH₄ on [Fe(PNP)Br₂]. Ruthenium complexes **3a-c** are active in acceptorless alcohol dehydrogenative coupling into ester under base-free conditions. From kinetic follow-up, the trend in initial activity is **3a** ≈ **3b** > [RuH(PNP)(BH₄)(CO)] >> **3c**; for robustness, [RuH(BH₄)(CO)(PNP)] > **3a** > **3b** >> **3c**. Hypotheses are given to account for the observed deactivation. Complexes **3b**, **3c**, **4a**, **4c**, **5c**, **7**, *cis*-**8** and **9** were characterized by X-ray crystallography.

Introduction

Over the recent years, catalytic processes based on the acceptorless dehydrogenative coupling concept have blossomed, affording novel and efficient access to a cornucopia of value-added products with high atom-economy and release of by-products such as water or hydrogen. Indeed, based on the metal-ligand cooperation concepts, new organometallic catalysts have been found to be active and selective in such transformations under very mild conditions.¹ For example, transition metal complexes supported by bifunctional ligands (along with ancillary monodentate ligands) have demonstrated impres-

sive activity towards the (de)hydrogenation and related hydrogen borrowing reactions,² thanks to pioneering works of Shvo,³ Noyori⁴ and Milstein.⁵ In the specific case of the systems based on pincer ligands, part of their efficiency stems from the relatively rigid tridentate coordination of these scaffolds, which stabilizes the metal center and induces higher catalyst robustness even under demanding conditions (high temperature, basic conditions etc.).⁶

To date, a fair number of bifunctional pincer ligands bearing coordinating atoms such as phosphorous,⁷ nitrogen,⁸ sulfur⁹ and carbenic carbon¹⁰ has been designed, aiming at tuning both electronic and steric properties.⁶ In contrast, only little attention has been paid to ancillary monodentate ligands within the metal coordination sphere.¹¹ As a matter of fact, CO appears to be a privileged ligand in this context, being involved in some of the most successful catalyst examples. It may be introduced from the starting carbonyl organometallic compound or it can be generated by decarbonylation reaction of alcohol under basic (catalytic) conditions. Interestingly, Gusev reported a series of complexes of general formula $[\text{Ru}(\text{Cl})_2(\text{L})(\text{NH}(\text{CH}_2\text{CH}_2\text{SEt})_2)]$ ($\text{L} = \text{CO}, \text{PPh}_3$ and AsPh_3) and found that among them, the complex bearing PPh_3 as ancillary ligand is the most active one for ester hydrogenation.⁹ Ogaka and Tayaki from Takasago Company replaced the carbonyl ligand within Ru-MACHO $[\text{RuXCl}(\text{L})(\text{PN}^{\text{H}}\text{P})]$ ($\text{X} = \text{H}, \text{Cl}, \text{PN}^{\text{H}}\text{P} = \text{NH}\{\text{CH}_2\text{CH}_2\text{P}(i\text{Pr})_2\}_2$) complexes by a σ -donor monodentate N-heterocyclic carbene ligand, thus allowing ester reduction under atmospheric hydrogen pressure.¹² On the other hand, Bernskoetter and Hazari have reported iron isonitrile PNP complexes, catalytically active for CO_2 hydrogenation to formate, though being less active than the analogous carbonyl derivative.¹³ Along these lines, Guan reported very recently on iron PNP isonitrile derivatives as efficient catalysts for ester hydrogenation.¹⁴ In the related field of carbonyl hydrogenation, both Reiser and Mezzetti demonstrated the interest of using isonitrile ligands to achieve efficient iron-based catalysis.¹⁵ Indeed, even if the catalytic transformations involving metal-isonitrile species are less studied than those of isoelectronic metal-carbonyl counterparts, advantages can be gained by the use of CNR-based catalysts¹⁶: Indeed, R groups on the CNRs allow for broad variation of their steric and electronic properties and of the strength of the M–C bonds, thus affecting the metal center electron density and catalytic behavior. Furthermore, similarly to carbonyl ligands, isonitrile ligands have distinctive IR and NMR signatures that contribute to both characterization and mechanistic studies.

As part of our ongoing program on structural and catalytic investigations around base-free dehydrogenative coupling reaction of alcohols,¹⁷ we investigated the synthesis of ruthenium and iron

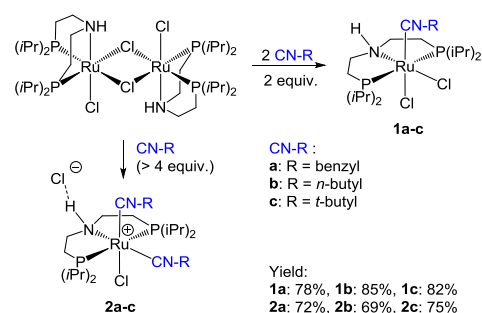
PNP supported complexes bearing isonitriles as ancillary ligand. These new isonitrile complexes were further catalytically assessed for base-free dehydrogenation reactions.

Results and Discussion

Dropwise addition of an isonitrile R-NC (**a**: R= CH₂Ph, **b**: R= *n*-Bu, **c**: *t*-Bu, 1.02-1.05 equiv. vs. Ru) THF solution to a suspension of Schneider's dimeric [RuCl(μ-Cl)(PN^HP)]₂ complex¹⁸ in THF afforded ruthenium isonitrile adducts [RuCl₂(CN-R)(PN^HP)] **1a-c** (Scheme 1). These complexes were formed along with small amount of cationic bis-isonitrile [Ru(Cl)(CN-R)₂(PN^HP)](Cl) complexes **2a-c** (1-5% from ³¹P NMR). Since [RuCl₂(CN-R)(PN^HP)] **1a-c** are less soluble in CH₂Cl₂ than both their ionic **2a-c** counterparts and the starting dimeric compound, their separation from the crude reaction mixture can be achieved by washing with CH₂Cl₂ at low temperature (-5 - 0 °C), with isolated yield ranging between 78 and 85%. Under similar conditions, performing the reaction in CH₂Cl₂ (in which both Schneider's dimer and **2a-c** are soluble) produced **1a-c** in a less selective manner, as higher amounts of **2a-c** were formed (up to 20% from ³¹P NMR). This is likely due to a competitive side-reaction of **1a-c** with isonitrile to form **2a-c** under such conditions. Indeed, complexes **2a-c** were prepared in good isolated yield (69-75%) by reaction of Schneider's complex or of **1a-c** with excess isonitrile, followed by crystallization in CH₂Cl₂/Et₂O at -20 °C. Both **1a-c** and **2a-c** series were characterized by multinuclear NMR (¹H, ³¹P, ¹³C, ¹⁵N) and IR spectroscopies and elemental analyses. Regarding species **1a-c**, the ³¹P NMR chemical shift of the PNP ligand of about 42 ppm is reminiscent of that of the PMe₃ adduct (41 ppm) which features a PNP bound in meridional coordination mode¹⁹. On the other hand, Bianchini, Peruzzini and coworkers reported the related isonitrile ruthenium complexes [RuCl₂(CN-R')(PN^{nPr}P)] (PN^{nPr}P= *n*Pr-N(CH₂CH₂PPh₂)₂),²⁰ in which the less bulky Ph-substituted PNP ligand adopts a facial type coordination mode. These give rise to ³¹P NMR signals at about 58 ppm. Bearing in mind that within the complexes of the isopropyl-substituted ligand ³¹P NMR chemical shifts are about 20 ppm higher than those of the phenyl substituted ligand complexes,^{17a} the values observed for **1a-c** are in line with a meridional coordination of the PNP ligand. However, as ³¹P chemical shift values are highly dependent on the nature of the trans ligand, care must be taken in assessing geometry based on these values only. Even if no single crystal was obtained for **1a-c** with quality allowing diffraction studies with publishable data, we succeeded in recording diffraction patterns for the **1a** complex. The overall coordination sphere could be assessed (See Electronic Supplementary Information). In this case, the PNP framework is indeed in

meridional configuration, the chloride ligands are located in mutually *cis* positions, and the isonitrile ligand is in the *cis* position compared to the ruthenium-bound amino moiety. This contrasts with previous observations on related complexes, where the ancillary ligand in $[\text{RuCl}_2(\text{PN}^{\text{R}}\text{P})(\text{L})]$ is in *trans* position from the Ru-N function.^{19,21}

Within the **1a-c** series, the presence of a N-H moiety was evidenced by the elongation vibration band at $3133\text{-}3148\text{ cm}^{-1}$ and by a triplet at 2.5-2.6 ppm on the ^1H NMR spectrum. Accordingly, 2D $\{^1\text{H}\text{-}^{15}\text{N}\}$ HSQC spectra of **1a-c** display signal at about 19 ppm, which is in line with sp^3 hybridization of the nitrogen center. Furthermore, the isonitrile ligands give rise to intense signals in the infrared spectrum at about 2100 cm^{-1} . According to $\{^1\text{H}\text{-}^{15}\text{N}\}$ HMBC experiments, characteristic ^{15}N NMR peaks assigned to the isonitrile function are observed in the 160-190 ppm range, thus being shifted highfield by 8-13 ppm from the corresponding free isonitriles' signal.²³ As a comparison, Bernskoetter and Hazari reported the analogous iron $[\text{FeCl}_2(\text{CN-R})(\text{PN}^{\text{H}}\text{P})]$, for which ^{31}P chemical shift and C-N IR absorption values are of about 65 ppm and 2050 cm^{-1} , respectively.¹³

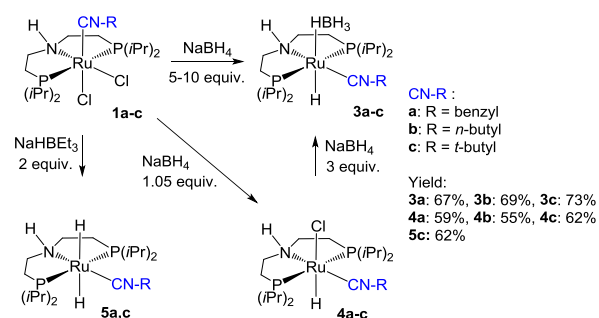


Scheme 1. Syntheses of Ru $\text{PN}^{\text{H}}\text{P}$ chloride isonitrile adducts.

The **2a-c** species afford spectral characteristics in line with the proposed structure as cationic species. ^{31}P NMR chemical shifts are found around 49 ppm, which is about 7 ppm higher than the values for **1a-c**. As a comparison, the ^{31}P chemical shift of the bis-carbonyl $[\text{RuCl}(\text{CO})_2(\text{PN}^{\text{H}}\text{P})](\text{BF}_4)$ derivative is of 49.8 ppm.²² The amino functionality spectroscopic features indicate that the chloride counter-anion interacts with the N-H via H-bonding. Namely, the $\nu(\text{N-H})$ in **2a** is found at about 70 cm^{-1} lower wavenumbers compared to that of **1a**, while the ^1H chemical shift of NH within **2a-c** is significantly low-field shifted by 4-5 ppm compared to that of **1a-c**. In agreement with the presence of two inequivalent isonitrile ligands, the $^1\text{H}\text{-}^{15}\text{N}$ HMBC spectrum of **2a-c** features two cross-signals in the 170-195 ppm ^{15}N chemical shift range. In the case of **2a**, on the 2D $^1\text{H}\text{-}^{13}\text{C}$ HMBC spectrum, two cross-peaks are detected

between the methylenic C≡N-CH₂ protons and the isonitrile N≡C carbon atoms (corresponding ¹H/¹³C pairs: 5.15/153.5 ppm and 4.90/160.1 ppm).²³

Treatment of **1a-c** with excess NaBH₄ (5 equiv.) in ethanol at room temperature led to the formation of borohydride complexes [RuH(BH₄)(RNC)(PN^HP)] (**3a-c**) in ~70% isolated yield after crystallization from toluene/*n*-pentane at -20 °C (Scheme 2). It is worth noting that the reaction of **1c** with NaBH₄ proceeds with lower rate than that of **1a** and **1b**. In this case, a longer reaction time (48 h instead of 14 h) is required to reach full conversion. This series of complexes displays spectroscopic properties similar to that of the related [RuH(BH₄)(CO)(PN^HP)] complex, with *inter alia* a ³¹P NMR chemical shift of about 78 ppm, and Ru-H resonating as a triplet centered at about -15 ppm (to be compared to 77.8 ppm and -13.5 ppm for the carbonyl complex, respectively). The κ¹-HBH₃ ligand resonates as a broad signal centered at about -1.5 ppm which is indicative of a rapid exchange between the BH₄ hydrogen atoms at room temperature. The presence of a N-H moiety was confirmed by both IR as well as ¹H and ¹H-¹⁵N HSQC NMR. Noteworthy, from the two-dimensional ¹H-¹H NOE experiment (NOESY), a correlation between the N-H and the Ru-HBH₃ peaks indicates a mutual *syn*-position of NH and Ru-HBH₃ moieties.



Scheme 2. General syntheses of Ru PN^HP hydride isonitrile complexes.

The solid-state structure of **3b** and **3c** was further determined by X-ray diffraction studies (Figures 1 and 2). Both adopt similar configuration, namely distorted octahedral coordination sphere, with a PNP framework in meridional configuration, the isocyanide being in the *trans*-position to the amino group. The borohydride and hydride groups are located in *syn*- and *anti*-position compared to the N-H bond, respectively. The isonitrile ligand adopts a nonlinear configuration, as evidenced by the C17-N2-C18 angle (**3b**: 163.23(13), **3c**: 160.70(13)°). It coordinates to the Ru(1) atom with a bond distance of 1.8944(10) and 1.8886(13) Å for **3b** and **3c** respectively, which is in the range of the Ru-C(isonitrile) distances of known isonitrile complexes of ruthenium (1.8–2.1 Å).²⁴ These complexes are isostructural to [RuH(BH₄)(CO)(PN^HP)],^{17a} the carbonyl and isonitrile ligands occupying the same coordination site.

The Ru-C bond distances of **3b** and **3c** are longer than the Ru-C bond distance (1.8389(12) Å) for [RuH(BH₄)(CO)(PN^HP)]. This is in line with a higher π-accepting character of the carbonyl ligand with respect to that of isonitrile ligands.¹³

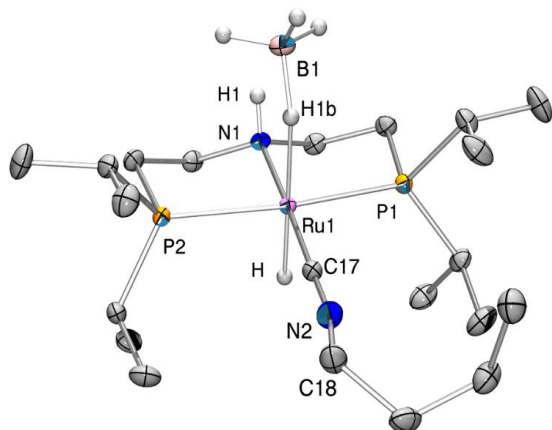


Figure 1. ORTEP of solid-state structure of **3b**. All H atoms (except the H on Ru, B and N) are omitted for clarity. Selected bond distances (Å): Ru1-P1 = 2.3092(3), Ru1-P2 = 2.3055(3), Ru1-N1 = 2.1884(9), Ru1-C17 = 1.8944(10), Ru1-H1B = 1.843(17), Ru1-H = 1.507(17), N2-C17 = 1.1779 (14). Selected angles (deg): P1-Ru1-H1B = 91.6(5), P1-Ru1-H = 89.7(6), P2-Ru1-P1 = 165.054(10), P2-Ru1-H1B = 92.8(5), P2-Ru1-H = 86.4(6), N1-Ru1-P1 = 82.71(2), N1-Ru1-P2 = 82.76(2), N1-Ru1-H1B = 93.8(5), N1-Ru1-H = 88.4(6), C17-Ru1-P1 = 97.69(3), C17-Ru1-P2 = 96.67(3), C17-Ru1-N1 = 177.36(4), C17-Ru1-H1B = 88.8(5), C17-Ru1-H = 89.0(6), H1B-Ru1-H = 177.6(8), C17-N2-C18 = 163.23(13).

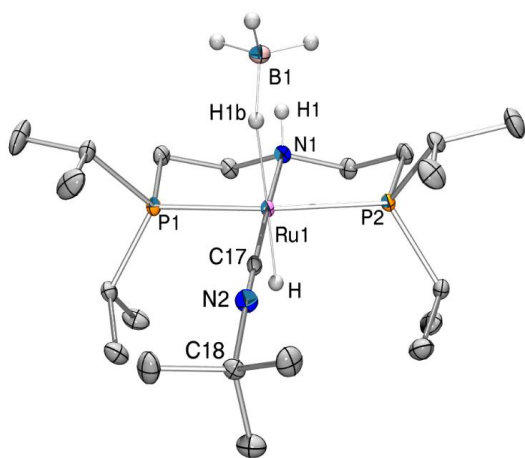


Figure 2. ORTEP of solid-state structure of **3c**. All H atoms (except the H on Ru, B and N) are omitted for clarity. Selected bond distances (Å): Ru1-P1 = 2.3089(3), Ru1-P2 = 2.3009(3), Ru1-N1 = 2.1914(11), Ru1-C17 = 1.8886(13), Ru1-H1B = 1.834(17), Ru1-H = 1.559(17). Selected angles (deg): P1-Ru1-H1B =

91.4(5), P1-Ru1-H = 88.7(6), P2-Ru1-P1 = 165.350(12), P2-Ru1-H1B = 93.4(5), P2-Ru1-H = 87.5(6), N1-Ru1-P1 = 82.85(3), N1-Ru1-P2 = 82.93(3), N1-Ru1-H1B = 95.3(5), N1-Ru1-H = 88.5(6), C17-Ru1-P1 = 97.25(4), C17-Ru1-P2 = 96.73(4), C17-Ru1-N1 = 176.51(5), C17-Ru1-H1B = 88.2(5), C17-Ru1-H = 88.0(6), H1B-Ru1-H = 176.3(8), C17-N2-C18 = 160.70(13).

Use of a stoichiometric quantity of NaBH₄ towards **1a-c** in EtOH allows to predominantly produce the hydrido-chloride [RuHCl(CN-R)(PN^HP)] species **4a-c**, along with small amount of **3a-c** (< 5%) (Scheme 2). Complexes **4a-c** can be obtained as pure products in 55-62% isolated yield range upon crystallization from a toluene/*n*-pentane mixture at -18 °C. As for the **3a-c** hydridoborohydride derivatives, these display NMR features similar to that of their carbonyl parent compound, [RuHCl(CO)(PN^HP)]. The isonitrile hydrido-chloride species ³¹P NMR chemical shift of about 74 ppm compares well to that of the CO derivative (75.8 ppm). In addition, the RuH ¹H NMR signal appears as triplet centered at about -17.5 ppm for **4a-c**, to be compared to -16.30 ppm for the carbonyl analogue. The retention of the N-H moiety is evidenced by the ν(N-H) at about 3170 cm⁻¹, and by the ¹⁵N NMR signal at about 54 ppm. This rules out the presence of cationic species [RuH(CN-R)(PN^HP)]⁺ with outer-sphere, H-bonded chloride counter-cation, as was observed in the case of the more sterically crowded [RuH(CO)(HN{CH₂CH₂P(*t*Bu)₂)₂}]⁺.^{17a}

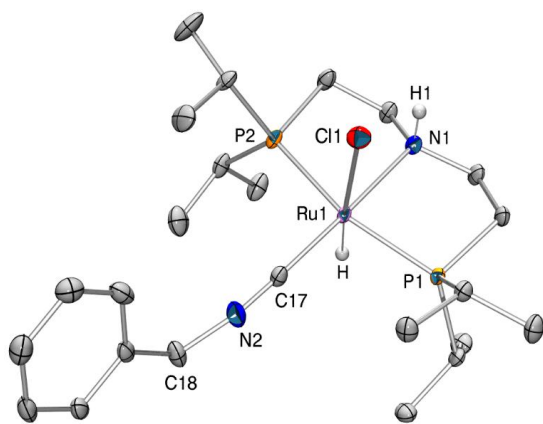


Figure 3. ORTEP of solid-state structure of **4a**. All H atoms (except the H on Ru and N) are omitted for clarity. Selected bond distances (Å): Ru1-P1 = 2.3225(4), Ru1-Cl1 = 2.5555(4), Ru1-P2 = 2.3050(4), Ru1-N1 = 2.1931(13), Ru1-C17 = 1.8819(16), Ru1-H = 1.56(2), N2-C17 = 1.179(2). Selected angles (deg): P1-Ru1-Cl1 = 88.995(13), P1-Ru1-H = 89.4(8), Cl1-Ru1-H = 173.5(8), P2-Ru1-P1 = 164.463(14), P2-Ru1-Cl1 = 92.044(14), P2-Ru1-H = 87.8(8), N1-Ru1-P1 = 82.71(3), N1-Ru1-Cl1 = 84.05(4), N1-Ru1-P2 = 81.98(3), N1-Ru1-H = 89.5(8), C17-Ru1-P1 = 100.38(5), C17-Ru1-Cl1 = 99.67(5), C17-Ru1-P2 = 94.73(5), C17-Ru1-N1 = 175.16(5), C17-Ru1-H = 86.8(8), C17-N2-C18 = 154.34(16).

This was confirmed by X-ray diffraction studies on **4a** and **4c** (Figures 3 and 4). These compounds adopt a distorted octahedral configuration, with the PNP ligand set in a meridional arrangement. Their structure is similar to that of above-described **3b** and **3c**, with the borohydride being formally substituted by a chloride ligand, or to that of the CO analogue, $[\text{RuHCl}(\text{CO})(\text{PN}^{\text{H}}\text{P})]$.

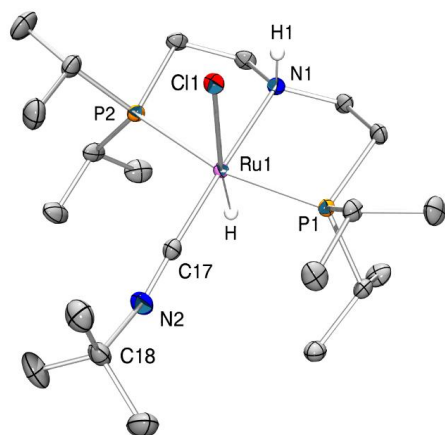


Figure 4. ORTEP of solid-state structure of **4c**. All H atoms (except the H on Ru and N) are omitted for clarity. Selected bond distances (Å): Ru1-Cl1 = 2.5426(3), Ru1-P1 = 2.3097(3), Ru1-P2 = 2.3071(3), Ru1-N1 = 2.1783(10), Ru1-C17 = 1.8831(13), Ru1-H = 1.588(17), N2-C17 = 1.1847(17). Selected angles (deg): Cl1-Ru1-H = 172.9(6), P1-Ru1-Cl1 = 89.589(12), P1-Ru1-H = 88.6(6), P2-Ru1-Cl1 = 90.372(12), P2-Ru1-P1 = 165.230(12), P2-Ru1-H = 89.6(6), N1-Ru1-Cl1 = 83.91(3), N1-Ru1-P1 = 82.92(3), N1-Ru1-P2 = 82.39(3), N1-Ru1-H = 89.0(6), C17-Ru1-Cl1 = 100.19(4), C17-Ru1-P1 = 96.96(4), C17-Ru1-P2 = 97.58(4), C17-Ru1-N1 = 175.90(5), C17-Ru1-H = 86.9(6), C17-N2-C18 = 154.91(14).

Reaction of **4a-c** with excess of NaBH_4 resulted in the formation of **3a-c** in quantitative manner based on ^1H and ^{31}P NMR (Scheme 2). The reaction of **1a** with 1.0 equiv. of NaHBET_3 affords the dihydride complex $[\text{RuH}_2(\text{CN-CH}_2\text{Ph})(\text{PN}^{\text{H}}\text{P})]$ **5a**, with a NMR yield of about 50%. Hydrido chloride derivative **4a** was not detected. This indicates that the reaction of **1a** with NaHBET_3 to form the intermediate **4a** takes place with lower rate than that of **4a** with NaHBET_3 to form **5a**, probably due to the higher solubility of intermediate **4a** with respect to the starting compound **1a**. Addition of 2 equiv. of NaHBET_3 to the suspension of **1a** resulted in the full conversion of the latter, affording **5a** as the main species, along with some unidentified hydride ruthenium products. Attempts to isolate **5a** as a pure product were unsuccessful as the compound suffers from low stability, affording unidentified species upon standing at room temperature in solution. Thus, **5a** was characterized *in-situ* by ^1H and ^{31}P NMR: Ru-H hydrides resonate as two triplets of doublets centered at -6.25 ($^2J_{\text{HH}} = 6.8$ Hz, $^2J_{\text{HP}} = 18.4$ Hz) and at -6.48 ($^2J_{\text{HH}} =$

6.9 Hz, $^2J_{\text{HP}} = 19.0$ Hz), while the $^{31}\text{P}\{^1\text{H}\}$ spectrum features a singlet at 86.89 ppm, in line with a structure featuring two equivalent phosphorus atoms.

Similar reaction with NaHBEt_3 was performed with **1c**, resulting in the formation of a mixture of two stereoisomeric compounds, meridional **mer-5c** and facial **fac-5c** of general formula $[\text{RuH}_2(\text{NC-}t\text{Bu})(\text{PN}^{\text{H}}\text{P})]$ in respective ratio of 1.5/1 with a cumulated isolated yield of 62% after crystallization from toluene/*n*-pentane at low temperature. The higher stability of **mer-5c/fac-5c** with respect to that of **5a** could be attributed to the bulkier nature of *t*-butyl groups that may stabilize the hydride species. As a comparison, Gusev isolated a structurally related *fac*- $[\text{RuH}_2(\text{PPh}_3)\{\text{HN}(\text{C}_2\text{H}_4\text{SEt})_2\}]$ complex.^{9a} Both **mer-5c** and **fac-5c** were characterized by multinuclear NMR spectroscopy and X-ray diffraction. For **mer-5c**, two inequivalent Ru-H hydrides resonate as one triplet of doublets centered at -6.86 ($^2J_{\text{HH}} = 4.9$ Hz, $^2J_{\text{HP}} = 18.0$ Hz) and one broadened triplet at -7.05 ppm ($^2J_{\text{HP}} = 19.0$ Hz) that are assigned to the Ru-H in *anti*- and *syn*-positions with respect to NH proton, respectively (Figure 5). The assignments are supported by the fact that such specific broadening in related bishydride complexes was observed and attributed to the presence and concentration of water in the sample.²⁵ The $^{31}\text{P}\{^1\text{H}\}$ spectrum displays a singlet at 84.78 ppm. The ^{15}N chemical shifts values were determined at 31.0 and 184.6 ppm for the NH and isonitrile functions, respectively. For the **fac-5c**, the two chemically equivalent Ru-H hydrides resonate as a multiplet centered at -8.82 ppm, being the AA' part of a AA'XX' system. The $^{31}\text{P}\{^1\text{H}\}$ spectrum displays a singlet at 74.08 ppm. The ^{15}N chemical shift values for the complex were determined at 19.5 and 178.0 ppm (assigned to NH and isonitrile functions, respectively) thanks to HSQC and HMBC experiments.

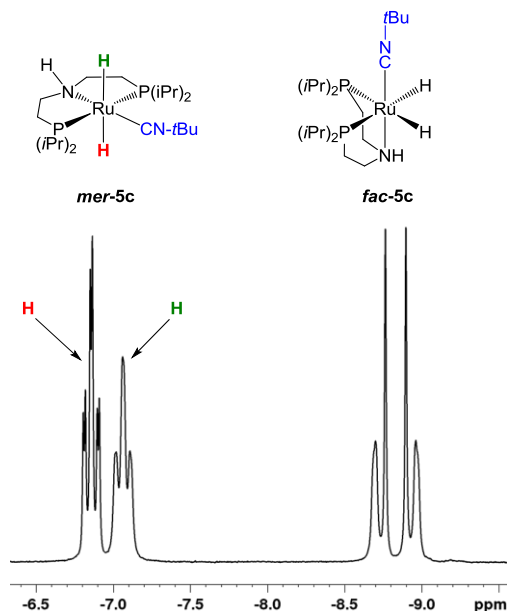


Figure 5. Hydride region of the ^1H NMR spectrum of the ***mer-5c/fac-5c*** mixture (400 MHz).

Though purification attempts were not met with success, due to thermal instability of the bishydride species, we succeeded in obtaining single crystals from a synthesis batch. Remarkably, both *mer* and *fac* isomers, ***mer-5c*** and ***fac-5c***, co-crystallized along with one molecule of NaBEt_4 . As seen on Figure 6, they thus form an entity where the two different ruthenium bishydride isomers assemble around a sodium cation, with tetraethylborate as non-interacting counteranion (Figure 6).²⁶ The two organometallic fragments arrange around the sodium so that the isonitrile ligands are organized in eclipsed, head-to-tail configurations. The ruthenium fragments both feature a distorted octahedral configuration. Within ***mer-5c***, the PNP ligand set binds to the metal center in a meridional arrangement. The *tert*-butylisonitrile ligand is in *trans* position with respect to the PNP framework's nitrogen. Accordingly, both hydrides (H_a and H_c on Figure 6) are in mutual *trans*-position. For ***fac-5c***, the PNP ligand set features a facial arrangement. The *tert*-butylisonitrile ligand is in *trans*-position with respect to the PNP's nitrogen. Both hydrides (H and H_b on Figure 6) are in mutual *cis* position. The Ru-C bond distance of ***mer-5c*** ($\text{Ru1-C17} = 1.871(4) \text{ \AA}$) is shorter than that of ***fac-5c*** ($\text{Ru2-C38} = 1.893(4) \text{ \AA}$). This owes in part to the interaction with the intercalated Na cation, which is preferentially interacting with the ***mer-5c*** framework. This reflects in the Na1-C17 and Na1-N2 distances of 2.619(4) and 2.671(4) \AA , respectively, which are shorter than the Na1-C38 and Na1-N4 distances of 2.784(4) and 3.297(5) \AA , respectively. The sodium is also stabilized by further interaction with the two mutually *cis* hydrides from ***mer-5c*** (Na1-H:

2.22(5) Å and Na1-Hb: 2.31(5) Å) and with a single hydride from **5c** with a significantly shorter Na1-Hc distance of 2.06(6) Å.

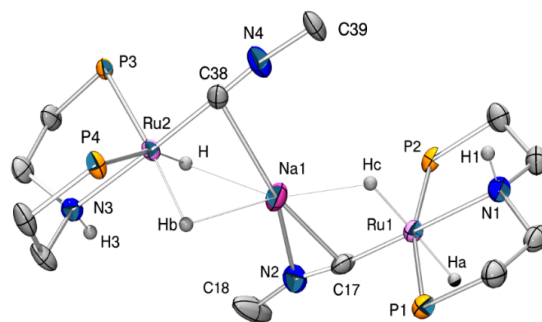
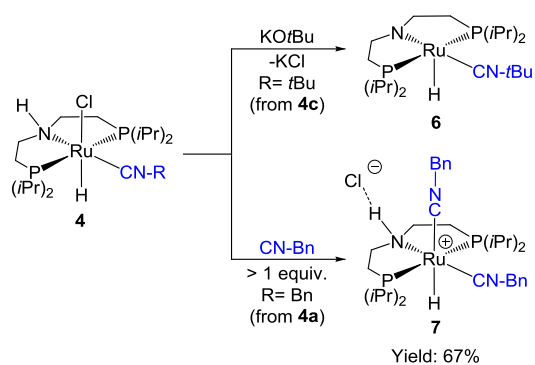


Figure 6. ORTEP of solid-state structure of the cation from **5c**·NaBEt₄. All H atoms (except those on Ru and N), *i*Pr groups on P, Me groups from *t*Bu moieties and the BEt₄⁻ anion are omitted for clarity. Selected bond distances (Å): **mer-5c**: Ru1-P2 = 2.2945(10), Ru1-P1 = 2.2942(11), Ru1-N1 = 2.218(3), Ru1-C17 = 1.871(4), Ru1-HA = 1.62(5), Ru1-Hc = 1.607(10), N2-C17 = 1.193(5). **fac-5c**: Ru2-P3 = 2.3208(9), Ru2-P4 = 2.3142(9), Ru2-N3 = 2.219(3), Ru2-C38 = 1.893(4), Ru2-H = 1.66(5), Ru2-Hb = 1.68(5), N4-C38 = 1.174(5). Selected angles (deg): **mer-5c**: P2-Ru1-Ha = 87.3(19), P2-Ru1-Hc = 94(3), P1-Ru1-P2 = 163.97(4), P1-Ru1-Ha = 85.4(19), P1-Ru1-Hc = 93(3), N1-Ru1-P2 = 82.15(9), N1-Ru1-P1 = 83.33(9), N1-Ru1-Ha = 87.9(19), N1-Ru1-Hc = 93(3), C17-Ru1-P2 = 98.04(12), C17-Ru1-P1 = 96.64(12), C17-Ru1-N1 = 178.68(15), C17-Ru1-Ha = 93.4(19), C17-Ru1-Hc = 86(3), Ha-Ru1-Hc = 178(3), C17-N2-C18 = 157.9(5). **fac-5c**: P3-Ru2-H = 81.0(16), P3-Ru2-Hb = 159.8(18), P4-Ru2-P3 = 110.82(3), P4-Ru2-H = 163.5(16), P4-Ru2-Hb = 84.3(18), N3-Ru2-P3 = 82.67(8), N3-Ru2-P4 = 82.25(9), N3-Ru2-Na1 = 117.01(9), N3-Ru2-H = 88.1(16), N3-Ru2-Hb = 86.3(18), C38-Ru2-P3 = 97.73(10), C38-Ru2-P4 = 94.48(11), C38-Ru2-N3 = 176.61(14), C38-Ru2-H = 95.3(16), C38-Ru2-Hb = 94.3(18), H-Ru2-Hb = 82(2), C38-N4-C39 = 171.6(4).

In analogy with the well-known chemistry of the hydrido chloro carbonyl derivatives, preparation of the amido species through N-H deprotonation of the hydrido chloro isonitrile species was attempted. Thus, reaction of **4c** with *t*BuOK (1.0 equiv.) was performed, leading to the formation of a new amido complex [RuH(CN-*t*Bu)(PNP)] (**6**, Scheme 3). Attempts to isolate this compound were unsuccessful, due to its low stability. Thus, formation of **6** was proposed based on in-situ NMR characterization: In the hydride region, the ¹H NMR spectrum displays a triplet centered at -18.74 ppm (²J_{HP} = 16.5 Hz). The ³¹P{¹H} NMR spectrum features a singlet at 91.8 ppm. In comparison, [RuH(CO)(PNP)] features ¹H and ³¹P NMR signals at -18.71 and 94.0 ppm; respectively. The fate of this complex remains undetermined, as decomposition into an unidentified mixture of products occurred.

In the presence of excess benzylnitrile, the hydrido chloride derivative **4a** reacts to afford the cationic species $[\text{RuH}(\text{CNCH}_2\text{Ph})_2(\text{PN}^{\text{H}}\text{P})]^+(\text{Cl}^-)$ (**7**, Scheme 3). The solid state structure of this complex was established by a single crystal X-rays diffraction study (Figure 7). **7** features a distorted octahedral geometry, with the PNP ligand in meridional configuration. The two isonitrile ligands occupy two mutually *cis*-positions, one being coordinated in the *trans* position amino group, and the other in *cis* position compared to the N-H functionality. Noteworthy, the (N1–H1...Cl1) distance of 2.433(2) Å and the corresponding angle (N1–H1...Cl1) of 164.8(1)° are indicative of a weak-strength hydrogen-bonding interaction involving (N–H...Cl) atoms.²⁷ In addition, the Ru1–C17 bond distance (2.0056(11) Å) is longer than the Ru1–C25 bond distance (1.9070(11) Å), likely due to the *trans*-influence of the hydride ligand exerted on the former.



Scheme 3. Reactivity examples of **4a** and **4c**

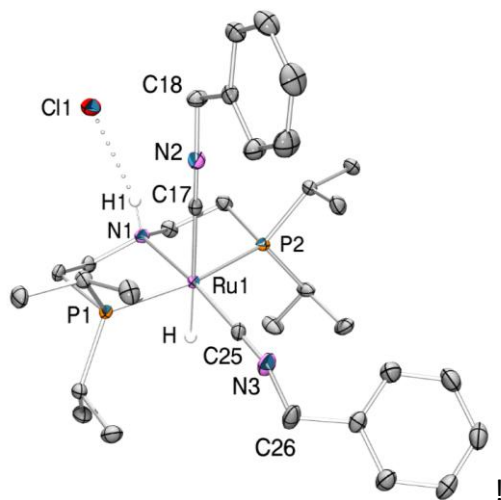


Figure 7. ORTEP of solid-state structure of **7**. All H atoms (except the H on Ru and N) are omitted for clarity. Selected bond distances (Å): Ru1–P1 = 2.3258(3), Ru1–P2 = 2.3287(3), Ru1–N1 = 2.1880(9), Ru1–C17 = 2.0056(11), Ru1–C25 = 1.9070(11), Ru1–H = 1.622(17), N2–C17 = 1.1609(15), N3–C25 =

1.1686(15). Selected angles (deg): P1-Ru1-P2 = 165.235(11), P1-Ru1-H = 88.5(6), P2-Ru1-H = 88.1(6), N1-Ru1-P1 = 82.68(3), N1-Ru1-P2 = 82.78(3), N1-Ru1-H = 86.8(6), C17-Ru1-P1 = 92.36(3), C17-Ru1-P2 = 90.04(3), C17-Ru1-N1 = 89.37(4), C17-Ru1-H = 175.9(6), C25-Ru1-P1 = 95.53(3), C25-Ru1-P2 = 98.66(3), C25-Ru1-N1 = 173.82(4), C25-Ru1-C17 = 96.62(5), C25-Ru1-H = 87.3(6), C17-N2-C18 = 175.61(12), C25-N3-C26 = 165.79(13).

Spectroscopic features of **7** are in line with this structure. On the ^1H NMR spectrum, the RuH and the N-H resonate at -8.48 and 8.43 ppm, respectively (Figure 8). The latter chemical shift (being severely low-field shifted compared to non-interacting NH moieties) combined with the $\nu(\text{N-H})$ band at 3055 cm^{-1} on the IR spectrum, is indicative of H-bonding between the amino hydrogen and the chloride atom.^{14a,28} Furthermore, the low field shift of this hydride peak stems from the strong *trans*-effect from the opposite axial isonitrile ligand. As a comparison, the ^1H chemical shift of the similar cationic bis-carbonyl $[\text{RuH}(\text{CO})_2(\text{PN}^{\text{H}}\text{P})]^+$ hydride is of -6.2 ppm.²⁹ ^1H - ^1H 2D NOESY experiment shows no through-space correlation between the Ru-H hydride peak and the N-H peak, indicating a mutually *anti*-arrangement of the Ru-H and N-H fragments. In addition, the presence of two different isonitrile ligands is evidenced by the two ^{15}N NMR signals at 172.8 and 159.4 ppm, and by the two $\nu(\text{C}\equiv\text{N})$ bands at 2135 and 2059 cm^{-1} on the infrared spectrum. The $^{13}\text{C}\{^1\text{H}\}$ spectrum displays two downfield triplets centered at 171.38 ($^2J_{\text{CP}} = 11.0\text{ Hz}$) and 157.42 ppm ($^2J_{\text{CP}} = 8.4\text{ Hz}$): The more downfield signal is attributed to the isonitrile carbon atom in *trans*-position with respect to the hydride ligand (*trans*-effect) while the less downfield one is assigned to the isonitrile carbon atom in *cis*-position to the hydride ligand. This is showed by comparison with the values of 160.0 and 153.5 ppm observed in **2a**: Formal substitution of the chloride by the hydride ligand causes a downfield shift of 11.38 ppm for the ^{13}C signal of the isonitrile ligand in *trans* position).

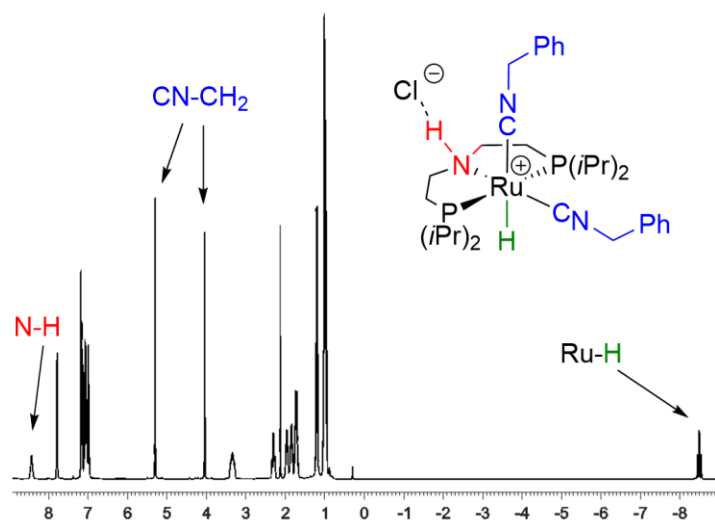


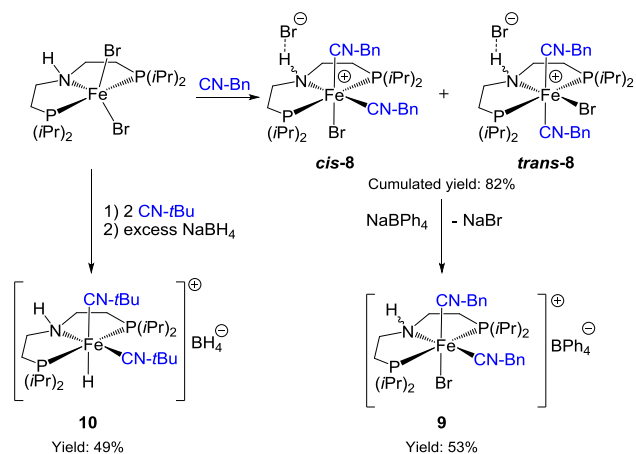
Figure 8. ^1H NMR spectrum of **7** (400 MHz, C_6D_6 , 300 K)

Bearing in mind the recent progresses on the use of Earth-abundant metal complexes as efficient catalysts in hydrogenation and dehydrogenation processes,^{6c,30} the analogous iron chemistry was also explored, following on the work of Hazari and collaborators on arylisonitrile PNP complexes.¹³ Synthetic studies were performed starting from the iron (II) complex $[\text{FeBr}_2(\text{PN}^{\text{H}}\text{P})]$.^{7d} In contrast to ruthenium chemistry, the reaction with benzylisonitrile (even upon addition of sub-equivalent quantities of isonitrile) exclusively lead to the formation of the ionic complex of formula $[\text{FeBr}(\text{CNCH}_2\text{Ph})_2(\text{PN}^{\text{H}}\text{P})]^+(\text{Br}^-)$ **8** (Scheme 4). Formation of a neutral mono-ligated isonitrile $[\text{FeBr}_2(\text{CNCH}_2\text{Ph})(\text{PN}^{\text{H}}\text{P})]$ complex was not observed. Under similar conditions, Hazari et al. reported the formation of a mixture of neutral dichloride $[\text{FeCl}_2(\text{CNAr})(\text{PN}^{\text{H}}\text{P})]$ and cationic monochloride $[\text{FeCl}(\text{CNAr})_2(\text{PN}^{\text{H}}\text{P})]^+(\text{Cl}^-)$ when starting from the less sterically crowded $[\text{FeCl}_2(\text{PN}^{\text{H}}\text{P})]$ derivative (chloride being smaller than bromide).^{13a} The chemistry of such isonitrile iron complexes was recently extended to $\text{CN}t\text{Bu}$ derivatives by Guan and coworkers, who thoroughly investigated *inter alia* the stereoselective issues during the synthesis of iron PNP complexes.^{14a}

Extensive NMR characterization studies on **8** revealed that there are actually two stereoisomers formed in 15.6/1 ratio: the major (*cis*-**8**) comprises two isonitrile ligands in mutually *cis*-position while the minor one (*trans*-**8**) has two isonitrile moieties in mutually *trans* position. The relevant ^{13}C NMR signals of isonitrile $\text{C}\equiv\text{N}$ carbons are determined at 171 and 166 ppm for *cis*-**8** and at 174 and 168 ppm for *trans*-**8**. The corresponding isonitrile nitrogen resonates at 188.7 and 183.5 ppm for *cis*-**8** and at 186.3 and 183.2 ppm for *trans*-**8**. Salt metathesis reaction of **8** with excess NaBPh_4 followed by recrystallization produced the complex $[\text{FeBr}(\text{CNCH}_2\text{Ph})_2(\text{PN}^{\text{H}}\text{P})]^+(\text{BPh}_4^-)$ **9** in moderate isolated yield (53%).³¹ The NH proton of *cis*-**8** resonates at lower field (6.51 ppm) with respect to that of **9** (2.40 ppm) which is in line with a (N-H \cdots Br) hydrogen bonding interaction in the former, and no H-bonding interaction in the latter. Accordingly, the $\nu(\text{N-H})$ of *cis*-**8** is found at about 165 cm^{-1} lower wavenumbers compared to that of **9** (3061 vs. 3227 cm^{-1} , respectively). The solid-state structure of *cis*-**8** and **9** were further determined by X-ray diffraction analysis (Figure 9 for *cis*-**8**; Figure 10 for **9** see Supporting Information). Complex *cis*-**8** features a distorted octahedral geometry with the PNP ligand in meridional configuration. Similarly to **7**, two isonitrile ligands occupy two mutually *cis*-positions. The (N1 \cdots Br2) and (N1-H1 \cdots Br2) distances of 3.355(4) and 2.487(4) Å, respectively, and the corresponding angle (N1-H1 \cdots Br2) of $168.82(3)^\circ$ are

indicative of a weak-strength hydrogen-bonding interaction involving (N–H···Br) atoms. The solid-state structure of **9** is very close to that of *cis*-**8**, except that, as the bromide counter-anion is replaced by tetraphenyl borate, the NH moiety is not involved in H-bonding interaction.

In order to access catalytically relevant hydride species, the reaction of **8** with excess of NaBH₄ was probed. It resulted in the formation of several unidentified complexes. Noteworthy, reaction of [FeBr₂(PN^HP)] with *t*-butylisocyanide and then with NaBH₄ resulted in the formation of a new hydride iron complex of formula [FeH(CN*t*Bu)₂(PN^HP)]⁺(BH₄⁻) **10** in 49% yield that was fully characterized by IR and NMR spectroscopies (Scheme 4). Guan recently described an ionic complex featuring the same cationic moiety as **10**, with BPh₄ as the counter-anion.^{14a} The ¹H and ³¹P{¹H} NMR spectra display a characteristic hydride signal as a triplet centered at -10.48 ppm (²J_{HP} = 50 Hz) and a singlet at 100.01 ppm, respectively. On the ¹¹B NMR spectrum, the free BH₄ anion resonates as a quintet centered at -38.9 ppm (¹J_{BH} = 82 Hz). ¹³C{¹H-³¹P} NMR spectrum displays two downfield signals at 175.4 and 166.2 ppm that are assigned to the two inequivalent C≡N carbon atoms from the equatorial and axial isocyanide ligands, respectively. Thanks to ¹H-¹⁵N HSQC and ¹H-¹⁵N HMBC measurements, ¹⁵N chemical shift values of NH and isocyanide functions were determined to be 31.7, 193.2 and 196.5 ppm, respectively.



Scheme 4. General syntheses of iron complexes.

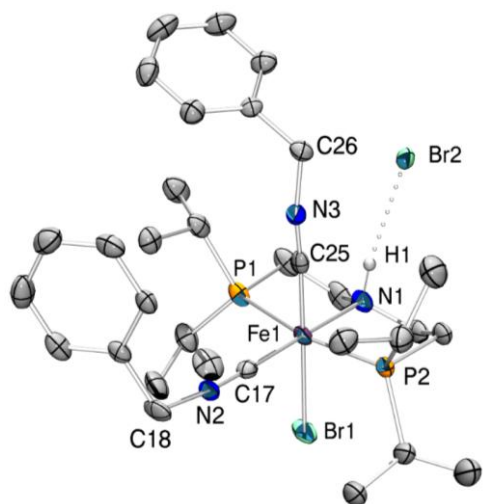


Figure 9. ORTEP of solid-state structure of *cis*-**8**. All H atoms (except the H on N) are omitted for clarity. Selected bond distances (Å): Br1-Fe1 = 2.4894(5), Fe1-P1 = 2.2804(9), Fe1-P2 = 2.2840(9), Fe1-N1 = 2.073(2), Fe1-C25 = 1.826(3), Fe1-C17 = 1.824(3), N2-C17 = 1.160(3), N3-C25 = 1.152(3). Selected angles (deg): P1-Fe1-Br1 = 91.33(3), P1-Fe1-P2 = 168.03(3), P2-Fe1-Br1 = 90.70(2), N1-Fe1-Br1 = 88.28(7), N1-Fe1-P1 = 84.06(8), N1-Fe1-P2 = 84.21(8), C25-Fe1-Br1 = 179.00(9), C25-Fe1-P1 = 88.29(9), C25-Fe1-P2 = 89.86(9), C25-Fe1-N1 = 92.60(11), C17-Fe1-Br1 = 89.69(8), C17-Fe1-P1 = 95.11(9), C17-Fe1-P2 = 96.70(9), C17-Fe1-N1 = 177.79(11), C17-Fe1-C25 = 89.42(12), C17-N2-C18 = 173.7(3), C25-N3-C26 = 169.2(3).

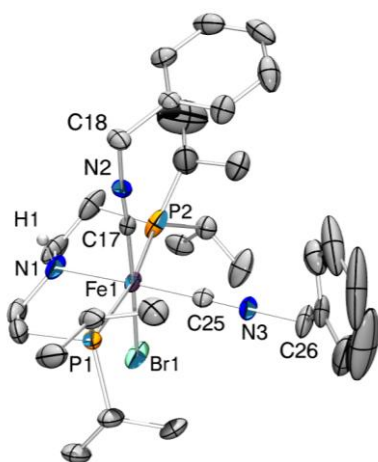


Figure 10. ORTEP of solid-state structure of **9**. BPh₄ anion and all H atoms (except the H on N) are omitted for clarity. Selected bond distances (Å): Br1-Fe1 = 2.5091(5), Fe1-P1 = 2.2726(10), Fe1-P2 = 2.2638(11), Fe1-N1 = 2.073(3), Fe1-C25 = 1.828(3), Fe1-C17 = 1.824(3), N2-C17 = 1.158(4), N3-C25 = 1.157(4). Selected angles (deg): P1-Fe1-Br1 = 90.22(3), P1-Fe1-P2 = 169.75(4), P2-Fe1-Br1 = 91.07(3),

N1-Fe1-Br1 = 88.72(8), N1-Fe1-P1 = 84.53(10), N1-Fe1-P2 = 85.32(10), C25-Fe1-Br1 = 88.83(9), C25-Fe1-P1 = 95.67(10), C25-Fe1-P2 = 94.52(10), C25-Fe1-N1 = 177.55(12), C17-Fe1-Br1 = 178.25(9), C17-Fe1-P1 = 89.03(10), C17-Fe1-P2 = 89.38(10), C17-Fe1-N1 = 89.63(12), C17-Fe1-C25 = 92.81(12), C17-N2-C18 = 175.7(3), C25-N3-C26 179.7(3).

Catalytic studies in alcohol acceptorless dehydrogenation

Complexes **3a-c** were further assessed in base-free dehydrogenative coupling of *n*-butanol into butyl butyrate. As a comparison, the carbonyl [RuH(BH₄)(CO)(PN^HP)] derivative was also evaluated under identical catalytic conditions. TON_{max} (maximal turnover number) and TOF₀ (initial turnover frequency) values were summarized in Table 1. It is worth noting that the cationic iron complex **9** is inactive for conversion of *n*-butanol into ester. Comparative kinetic profiles of *n*-butanol conversion into ester are presented on Figure 11. Interestingly, complexes **3a** (TOF₀ = 6220 h⁻¹) and **3b** (TOF₀ = 5970 h⁻¹) bearing respectively benzyl and *n*-butyl isonitrile were found to be initially more active than the benchmark carbonyl complex (TOF₀ = 4300 h⁻¹). However, the latter is catalytically more robust: Its corresponding TON_{max} value (14100) is higher than that of **3a** (10200) and **3b** (9000). These isonitrile adducts reach a plateau after about 3 hours of reaction, which may indicate catalyst deactivation. On the other hand, the *t*Bu isonitrile derivative reaches its deactivated regime after about one hour, totaling about 2900 TON. These reactivity patterns illustrate that the substitution of the carbonyl by the isonitrile ligand has a beneficial effect. Catalytic behavior is indeed modulated by the nature of the isonitrile substituent. Thus, according to TOF₀ and TON_{max} values, the catalytic activity and robustness can be classified as follows: for catalytic activity, **3a** ≈ **3b** > [RuH(BH₄)(CO)(PN^HP)] >> **3c**; for robustness, [RuH(BH₄)(CO)(PN^HP)] > **3a** > **3b** >> **3c**. Considering that the bulky *t*-butyl group is rather remote from the metal center, it is doubtful that the lowest catalytic performance of **3c** is related to steric effects. The origin of this behavior may be found in the more donating character of the *t*-butyl-substituted isonitrile, or to deactivation pathways specific to this ligand. The kinetic profile recorded for the *t*-butylisonitrile precatalyst (Figure 11) hints at a behavior different from that of its benzyl and *n*-butyl counterparts, reaching a plateau after about 90 minutes and achieving less than 3000 turnover numbers. As reported by Walton and Jones, complexes featuring this specific ligand can thermally decompose into cyanide derivatives, with release of isobutene or isobutane.³² In the present case, this would result in formation of complexes featuring Ru-CN groups. However, spectroscopic investigations on

reaction mixtures did not allow us to identify such species. More generally, the lesser robustness of the isonitrile derivatives compared to that of their carbonyl counterpart may be ascribed to known reactivity patterns of metal-coordinated isonitrile ligands, such as Ru-H insertion into coordinated C≡N- or nucleophilic attack on the Ru-C≡N- carbon by the alcohol substrate.^{33,34,35,36}

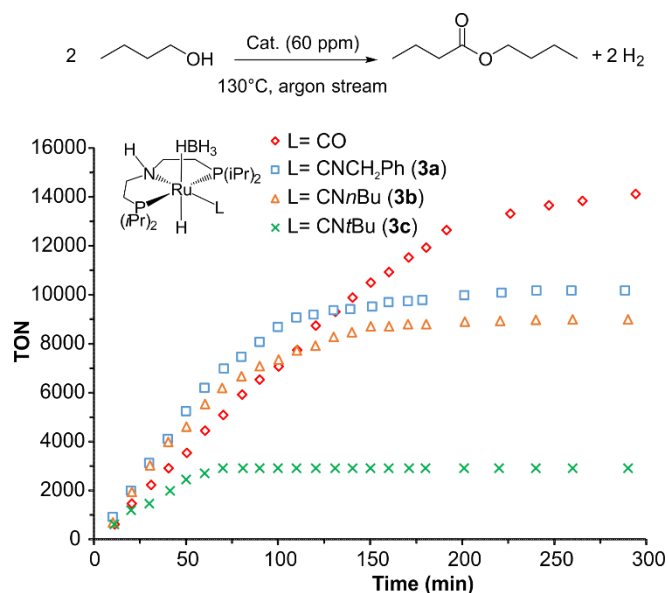


Figure 11. Comparative kinetic profiles of butanol conversion mediated by Ru PNP complexes. Conditions: Ru loading = 60 ppm, T = 130 °C.

Table 1. TON_{max} and TOF° values for butanol conversion to butyl butyrate.

Complexes	TOF°(h ⁻¹)	TON	Conversion (%) ^a
3a	6220	10200	61
3b	5970	9000	54
3c	2930	2900	17
[RuH(BH ₄)(CO)(PN ^H P)]	4300	14100	85
9c	0	0	0

Conditions: Ru loading = 60 ppm, T = 130 °C. ^a: measured by ¹H NMR

Conclusions

A series of neutral and cationic ruthenium and iron aliphatic PNP-type pincer complexes bearing benzyl, *n*-butyl or *tert*-butyl isocyanides as ancillary ligands have been prepared. Their structure was inves-

tigated notably by multinuclear NMR spectroscopy, as well as by single crystal X-ray diffraction studies. Borohydride ruthenium isonitrile complexes, structurally similar to the benchmark Ru-MACHO-BH carbonyl derivative, were catalytically evaluated for base-free acceptorless dehydrogenative coupling reactions (ADC) of butanol. Catalytic activities were found to be related to the nature of isonitrile bound to the metal center, as shown by kinetic follow-up. Although their initial catalytic activity is better or comparable to that of the carbonyl parent compound, the robustness of [Ru]-CNR bond may be compromised under catalytic reaction conditions, undergoing decomposition to afford inactive species. While these results with isonitrile-containing systems bring positive elements for catalytic activity improvement of Ru PNP systems, the future implementation of this class of ancillary ligands is bound to the understanding of the deactivation pattern(s), and to the possibility to shut down such pathway(s). This will be the focus of future studies.

Experimental Section

All experiments were carried out under argon atmosphere using a glovebox or a vacuum line using standard Schlenk techniques unless some special conditions are pointed out. All ruthenium and iron complexes and tridentate ligands were stored under argon. $[\text{Ru}(\text{Cl})(\mu\text{-Cl})(\text{PN}^{\text{H}}\text{P})_2]$ ¹⁸ and $[\text{FeBr}_2(\text{PN}^{\text{H}}\text{P})]$ ^{7d,37} were prepared according to literature procedures. ¹H, ¹³P, ¹³C, ¹⁵N and ¹¹B NMR spectra were recorded at 300 K on a Bruker Avance 300 and 400 NMR spectrometers. ¹H and ¹³C NMR chemical shifts are reported in ppm (δ) downfield from tetramethylsilane. ³¹P NMR chemical shifts are reported in ppm (δ) downfield from H₃PO₄. ¹⁵N NMR chemical shift are reported in ppm (δ) downfield from NH₃, and were indirectly determined from 2D ¹H-¹⁵N HMBC/HSQC. ¹¹B NMR chemical shift are reported in ppm (δ) downfield from BF₃.Et₂O. Common abbreviations used in the NMR experiments are as follows: s singlet (s), doublet (d), triplet (t), virtual triplet (vt), quartet (q), quintet (qt), multiplet (m). IR spectra were recorded on a Nicolet 6700 FT-IR spectrometer equipped with a Praying Mantis mirror chamber (from Harrick Scientific) by using a DRIFT cell equipped with KBr windows. The samples were prepared under argon in a glovebox. Typically, 64 scans were accumulated for each spectrum (resolution 4 cm⁻¹). Data are reported as follows: weak (w), medium (m), strong (s) and very strong (vs).

[RuCl₂(CN-CH₂Ph)(PN^HP)] (1a). To the yellow-orange suspension of dimeric $[\text{Ru}(\text{Cl})(\mu\text{-Cl})(\text{PN}^{\text{H}}\text{P})_2]$ complex (1.38 g, 1.45 mmol) in THF (50 mL) was added dropwise a solution of benzyl isocyanide (2.1 equiv., 0.35 mL) in THF (10 mL) at room temperature. The mixture was stirred for 14h at RT, affording an off-white suspension. The reaction mixture was evaporated under reduced pressure to give an off-white

solid, which was further washed with small amounts of CH_2Cl_2 at 0 °C (5 x 3 mL) and then with *n*-pentane (3 x 20 mL) and finally dried under high vacuum. Yield: 1.35 g, 78%. Anal. Calcd. for $\text{C}_{24}\text{H}_{44}\text{Cl}_2\text{N}_2\text{P}_2\text{Ru}$: C 48.48; H 7.46; N 4.71. Found: C 48.32; H 7.37; N 4.64. FT-IR (cm^{-1}): 3133 (s, $\nu_{\text{N-H}}$), 2105 (vs, $\nu_{\text{C}\equiv\text{N}}$). ^1H NMR (298 K, CD_2Cl_2 , 400.33 MHz, ppm): δ 7.45-7.26 (m, 5H, $\text{C}_{\text{Ar-H}}$, PhCH_2NC), 4.88 (s, 2H, PhCH_2NC), 3.19 (m, 2H, CH *iPr*), 3.01 (m, 2H, CH_2 PNP), 2.66 (m, 2H, CH_2 PNP), 2.54 (brt, 1H, NH PNP), 2.38 (m, 2H, CH *iPr*), 2.24 (m, 2H, CH_2 PNP), 1.51 (dt, 6H, $J_{\text{HH}} = 7.4$ Hz, $J_{\text{HP}} = 7.4$ Hz, CH_3 *iPr*), 1.40 (dt, 6H, $J_{\text{HH}} = 7.4$ Hz, $J_{\text{HP}} = 7.4$ Hz, CH_3 *iPr*), 1.36 (dt, 6H, $J_{\text{HH}} = 7.2$ Hz, $J_{\text{HP}} = 6.5$ Hz, CH_3 *iPr*), 1.30 (dt, 6H, $J_{\text{HH}} = 7.2$ Hz, $J_{\text{HP}} = 6.9$ Hz, CH_3 *iPr*), 1.23 (m, 2H, CH_2 PNP). $^{13}\text{C}\{^1\text{H}\}$ NMR (298 K, CD_2Cl_2 , 100.663 MHz, ppm): δ 134.14 ($\text{CH}_2\text{C}_{\text{Ar}}$), 129.19, 128.28, 127.52 ($\text{C}_{\text{Ar-H}}$), 56.1, 51.4 (CH_2 PNP), 49.3 (CH_2 , PhCH_2NC), 29.2 (CH *iPr*), 28.0, 27.0 (CH_2 PNP), 25.2, 23.0 (CH *iPr*), 19.9, 19.7, 19.0 (CH_3 *iPr*). $^{31}\text{P}\{^1\text{H}\}$ NMR (298 K, CD_2Cl_2 , 162.057 MHz, ppm): δ 42.37. 2D $\{^1\text{H}-^{15}\text{N}\}$ HSQC NMR (298 K, CD_2Cl_2 , 40.565 MHz, ppm): δ 19.1 (NH PNP). 2D $\{^{15}\text{N}-^1\text{H}\}$ HMBC NMR (298 K, CD_2Cl_2 , 40.565 MHz, ppm): δ 164.1 (PhCH_2NC).

[RuCl₂(CN-*n*Bu)(PN^HP)] (1b). The complex was prepared in a similar manner to the procedure described above for **1a**. Yield: 1.38 g, 85%. Anal. Calcd. for $\text{C}_{21}\text{H}_{46}\text{Cl}_2\text{N}_2\text{P}_2\text{Ru}$: C 45.00; H 8.27; N 5.00. Found: C 45.16; H 8.63; N 5.14. FT-IR (cm^{-1}): 3146 (s, $\nu_{\text{N-H}}$), 2101 (vs, $\nu_{\text{C}\equiv\text{N}}$). ^1H NMR (293K, CD_2Cl_2 , 400.33 MHz, ppm): δ 3.68 (t, 2H, $^3J_{\text{HH}} = 6.8$ Hz, $\text{CNCH}_2(\text{CH}_2)_2\text{CH}_3$), 3.21 (m, 2H, CH *iPr*), 2.98 (m, 2H, CH_2 PNP), 2.75-2.52 (m, 3H, CH_2 PNP and NH), 2.45 (m, 2H, CH *iPr*), 2.25 (m, 2H, CH_2 PNP), 1.62 (m, 2H, $\text{CN-CH}_2\text{CH}_2\text{CH}_2\text{CH}_3$), 1.55-1.21 (m, 4H, $\text{CN-(CH}_2)_2\text{CH}_2\text{CH}_3$ and CH_2 PNP), 1.51 (m, 6H, CH_3 *iPr*), 1.49 (m, 6H, CH_3 *iPr*), 1.38 (m, 6H, CH_3 *iPr*), 1.36 (m, 6H, CH_3 *iPr*), 0.93 (t, 3H, $J_{\text{HH}} = 7.3$ Hz, $\text{CN(CH}_2)_3\text{CH}_3$). $^{31}\text{P}\{^1\text{H}\}$ NMR (298 K, CD_2Cl_2 , 162.057 MHz, ppm): δ 42.76 (PNP). $^{13}\text{C}\{^1\text{H}\}$ NMR (298 K, C_6D_6 , 100.663 MHz, ppm): δ 51.6 (t, $J_{\text{CP}} = 2.9$ Hz, CH_2 PNP), 45.6 ($\text{CNCH}_2(\text{CH}_2)_2\text{CH}_3$), 33.2 (CH_2), 29.04 (d, $J_{\text{CP}} = 10$ Hz, CH *iPr*), 28.3 (t, $J_{\text{CP}} = 8.7$ Hz, CH_2 PNP), 23.09 (d, 2C, $J_{\text{CP}} = 8.9$ Hz, CH *iPr*), 20.4 (CH_2), 20.3, 20.2, 20.1, 19.3 (CH_3 *iPr*), 14.3 ($\text{CNCH}_2(\text{CH}_2)_2\text{CH}_3$). 2D $\{^{15}\text{N}-^1\text{H}\}$ HSQC NMR (298 K, CD_2Cl_2 , 40.565 MHz, ppm): δ 18.5 (NH PNP). 2D $\{^{15}\text{N}-^1\text{H}\}$ HMBC NMR (298 K, CD_2Cl_2 , 40.565 MHz, ppm): δ 162.5 ($\text{CN(CH}_2)_3\text{CH}_3$).

[RuCl₂(CN-*t*Bu)(PN^HP)] (1c). The complex was prepared in a similar manner to the procedure described above, though with a reaction time of 48 hours. Yield: 1.33 g, 82%. Anal. Calcd. for $\text{C}_{21}\text{H}_{46}\text{Cl}_2\text{N}_2\text{P}_2\text{Ru}$: C 45.00; H 8.27; N 5.00. Found: C 44.92; H 8.29; N 4.95. FT-IR (cm^{-1}): 3148 (s, ν_{NH}), 2102 (s, $\nu_{\text{C}\equiv\text{N}}$). ^1H NMR (298 K, CD_2Cl_2 , 400.33 MHz, ppm) δ 3.19 (m, 2H, CH *iPr*), 2.99 (m, 2H, CH_2 PNP), 2.66 (m, 2H, CH_2 PNP), 2.52 (m, 2H, CH *iPr*), 2.47 (1H, brt, $J_{\text{HH}} = 12.2$, 4.0 Hz, NH), 2.30 (m, 2H, CH_2 PNP), 1.56 (m, 6H, CH_3 *iPr*), 1.53 (m, 6H, CH_3 *iPr*), 1.42 (s, 9H, CH_3 *t*Bu), 1.40 (m, 6H, CH_3 *iPr*), 1.37 (m, 6H, CH_3 *iPr*), 1.22 (m, 2H, CH_2

PNP). $^{31}\text{P}\{^1\text{H}\}$ NMR (298 K, CD_2Cl_2 , 162.057 MHz, ppm): δ 42.06 (PNP). $^{13}\text{C}\{^1\text{H}\}$ NMR (298 K, CD_2Cl_2 , 100.663 MHz, ppm): δ 51.27 (t, $J_{\text{CP}} = 2.9$ Hz, CH_2 PNP), 31.75 (s, CH_3 *t*Bu), 29.80 (t, $J_{\text{CP}} = 10.4$ Hz, CH *i*Pr), 28.35 (t, $J_{\text{CP}} = 8.8$ Hz, CH_2 PNP), 22.93 (t, $J_{\text{CP}} = 7.9$ Hz, CH *i*Pr), 20.18 (CH_3 *i*Pr), 19.90 (CH_3 *i*Pr), 19.49 (CH_3 *i*Pr), 19.44 (CH_3 *i*Pr). 2D $\{^{15}\text{N}-^1\text{H}\}$ HSQC NMR (298 K, CD_2Cl_2 , 40.565 MHz, ppm): δ 19.1 (NH, PNP). 2D $\{^{15}\text{N}-^1\text{H}\}$ HMBC NMR (298 K, CD_2Cl_2 , 40.565 MHz, ppm): δ 187.7 (CN-*t*Bu).

[RuCl(CN-CH₂Ph)₂(PN^HP)](Cl) (2a). To a yellow-orange solution of dimeric $[\text{Ru}(\text{Cl})(\mu\text{-Cl})(\text{PN}^{\text{H}}\text{P})_2]$ complex (1.0g, 1.05 mmol) in CH_2Cl_2 (50 mL) was added dropwise a solution of benzyl isocyanide (5.6 equiv.) in CH_2Cl_2 (10 mL) at room temperature. The reaction mixture immediately turns to green. After stirring for 20h at RT, a pale yellow suspension was obtained. The reaction mixture was evaporated to dryness. The obtained residual solid was washed with diethyl ether (3x5 mL) and *n*-pentane (3x5mL) and dried under vacuum. The product was further purified by crystallization into CH_2Cl_2 /diethyl ether at -20 °C as a white solid. Yield: 1.08 g, 72%. The complex can also be synthesized by using THF as solvent. Anal. Calcd. for $\text{C}_{32}\text{H}_{51}\text{Cl}_2\text{N}_3\text{P}_2\text{Ru}$: C 54.01; H 7.22; N 5.90. Found: C 54.2; H 7.91; N 6.10. FT-IR (cm^{-1}): 3062 (m, ν_{NH}), 2140 (vs, $\nu_{\text{C}\equiv\text{N}}$). ^1H NMR (298 K, CD_2Cl_2 , 400.33 MHz, ppm): δ 7.69 (m, 2H, $\text{C}_{\text{Ar}}\text{-H}$, Ph), 7.46-7.31 (m, 8H, $\text{C}_{\text{Ar}}\text{-H}$, Ph), 6.91 (brt, 1H, $J_{\text{HH}} = 9.8, 4.1$ Hz, NH), 5.15 (s, 2H, CH_2Ph), 4.90 (s, 2H, CH_2Ph), 3.02 (m, 2H, CH_2 PNP), 2.33 (m, 2H, CH *i*Pr), 2.30 (m, 2H, CH *i*Pr), 2.06 (m, 2H, CH_2 PNP), 1.95 (m, 2H, CH_2 PNP), 1.83 (m, 2H, CH_2 PNP), 1.28 (dt, 6H, $J_{\text{HH}} = 7.5$ Hz, $J_{\text{HP}} = 7.4$ Hz, CH_3 *i*Pr), 1.27 (dt, 6H, $J_{\text{HH}} = 7.3$ Hz, $J_{\text{HP}} = 7.4$ Hz, -CH_3 , *i*Pr), 1.26 (dt, 6H, $J_{\text{HH}} = 7.1$ Hz, $J_{\text{HP}} = 7.2$ Hz, CH_3 *i*Pr), 1.15 (dt, 6H, $J_{\text{HH}} = 7.1$ Hz, $J_{\text{HP}} = 6.9$ Hz, CH_3 *i*Pr). $^{31}\text{P}\{^1\text{H}\}$ NMR (298 K, CD_2Cl_2 , 121.495 MHz, ppm): δ 48.77 (PNP). $^{13}\text{C}\{^1\text{H}\}$ NMR (298 K, CD_2Cl_2 , 100.663 MHz, ppm): δ 135.50 (C_{Ar} quat., Ph), 132.93 (C_{Ar} quat., Ph), 129.58 ($\text{C}_{\text{Ar}}\text{-H}$, Ph), 129.31 ($\text{C}_{\text{Ar}}\text{-H}$, Ph), 129.25 ($\text{C}_{\text{Ar}}\text{-H}$, Ph), 128.89 ($\text{C}_{\text{Ar}}\text{-H}$, Ph), 128.10 ($\text{C}_{\text{Ar}}\text{-H}$, Ph), 56.17 (CH_2 PNP), 49.29 (CH_2Ph), 49.13 (CH_2Ph), 30.68 (t, $J_{\text{CP}} = 11.8$ Hz, CH_2 PNP), 28.11 (t, 2C, $J_{\text{CP}} = 11.1$ Hz, CH *i*Pr), 26.12 (t, $J_{\text{CP}} = 8.9$ Hz, CH *i*Pr), 19.88 (CH_3 *i*Pr), 19.52 (CH_3 *i*Pr), 19.20 (CH_3 *i*Pr), 19.17 (CH_3 *i*Pr). 2D $\{^1\text{H}-^{13}\text{C}\}$ HMBC NMR (298 K, CD_2Cl_2 , 100.663 MHz): 160.0, 153.5 (CN- CH_2Ph). 2D $\{^{15}\text{N}-^1\text{H}\}$ HSQC NMR (298 K, CD_2Cl_2 , 40.565 MHz, ppm): δ 16.37 (NH, PNP). 2D $\{^{15}\text{N}-^1\text{H}\}$ HMBC NMR (293K, CD_2Cl_2 , 40.565 MHz, ppm): δ 173.91 (CN CH_2Ph), 171.37(CN CH_2Ph).

[RuCl(CN-*n*Bu)₂(PN^HP)](Cl) (2b). The complex was prepared in a similar manner to the procedure described above for **2a**. Yield: 69%. Anal. Calcd. for $\text{C}_{26}\text{H}_{55}\text{Cl}_2\text{N}_3\text{P}_2\text{Ru}$: C 48.52; H 8.61; N 6.53. Found: C 48.63; H 9.25; N 7.08. ^1H NMR (298 K, C_6D_6 , 400.33 MHz, ppm): δ 6.80 (brt, 1H, $J_{\text{HH}} = 10, 4.7$ Hz, NH), 3.87 (t, 2H, $J_{\text{HH}} = 6.9$ Hz, CN $\text{CH}_2(\text{CH}_2)_2\text{CH}_3$), 3.70 (t, 2H, $J_{\text{HH}} = 6.9$ Hz, CN $\text{CH}_2(\text{CH}_2)_2\text{CH}_3$), 3.01 (m, 2H, CH_2

PNP), 2.55 (m, 2H, CH *i*Pr), 2.48 (m, 2H, CH *i*Pr), 2.10 (m, 2H, CH₂ PNP), 1.97 (m, 2H, CH₂ PNP), 1.86 (m, 2H, CH₂ PNP), 1.71 (m, 4H, CH₂), 1.49 (m, 6H, CH₃ *i*Pr), 1.46 (m, 4H, CH₂), 1.42 (m, 6H, CH₃ *i*Pr), 1.39 (m, 6H, CH₃ *i*Pr), 1.33 (m, 6H, CH₃ *i*Pr), 0.93 (t, 3H, $J_{\text{HH}} = 7.3$ Hz, CNCH₂(CH₂)₂CH₃), 0.92 (t, 3H, $J_{\text{HH}} = 7.4$ Hz, CNCH₂(CH₂)₂CH₃). ³¹P{¹H} NMR (298 K, C₆D₆, 121.495 MHz, ppm): δ 49.9 (PNP). ¹³C{¹H} NMR (298 K, C₆D₆, 100.663 MHz, ppm): δ 55.94 (CH₂ PNP), 44.98 (CH₂, *n*Bu), 44.70 (CH₂ *n*Bu), 31.38 (CH₂ *n*Bu), 30.97 (CH₂ *n*Bu), 30.38 (t, $J_{\text{CP}} = 11.3$ Hz, CH *i*Pr), 27.92 (t, $J_{\text{CP}} = 10.4$ Hz, CH₂ PNP), 25.90 (t, $J_{\text{CP}} = 9.3$ Hz, CH *i*Pr), 20.06 (CH₂ *n*Bu), 19.98 (CH₂ *n*Bu), 19.86 (CH₃ *i*Pr), 19.58 (CH₃ *i*Pr), 19.20 (CH₃ *i*Pr), 13.36 (CH₃ *n*Bu), 13.21 (CH₃, *n*Bu). 2D {¹⁵N-¹H} HSQC NMR (298 K, C₆D₆, 40.565 MHz, ppm): δ 17.8 (NH, PNP). 2D {¹⁵N-¹H} HMBC NMR (298 K, C₆D₆, 40.565 MHz, ppm): δ 176.0, 171.8 (CN(CH₂)₃CH₃).

[RuCl(CN-*t*Bu)₂(PN^HP)]Cl (2c). The complex was prepared in a similar manner to the procedure described above for **2a**. Yield: 75%. Anal. Calcd. for C₂₆H₅₅Cl₂N₃P₂Ru: C 48.52; H 8.61; N 6.53. Found: C 48.63; H 9.25; N 7.08. ¹H NMR (300 K, CD₂Cl₂, 400.33 MHz, ppm): δ 6.74 (br, t, 1H, $J_{\text{HH}} = 10.4$ Hz, NH PNP), 3.03 (m, 2H, CH₂ PNP), 2.60 (m, 2H, CH *i*Pr), 2.50 (m, 2H, CH *i*Pr), 2.15 (m, 2H, CH₂ PNP), 1.92 (m, 2H, CH₂ PNP), 1.8 (m, 2H, CH₂ PNP), 1.56 (s, 9H, CH₃ *t*Bu), 1.53 (m, 6H, CH₃ *i*Pr), 1.49 (m, 6H, CH₃ *i*Pr), 1.48 (s, 9H, CH₃ *t*Bu), 1.41 (dt, 6H, $J_{\text{HH}} = 7.5$ Hz, $J_{\text{HP}} = 6.9$ Hz, CH₃ *i*Pr), 1.34 (dt, 6H, CH₃, $J_{\text{HH}} = 7.5$ Hz, $J_{\text{HP}} = 6.9$ Hz, CH₃ *i*Pr). ³¹P{¹H} NMR (300 K, CD₂Cl₂, 400.33 MHz, ppm): δ 49.07 (PNP). ¹³C{¹H} NMR (300 K, CD₂Cl₂, 100.663 MHz, ppm): δ 57.53 (d, C quat. *t*Bu), 57.40 (d, C quat. *t*Bu), 55.62 (CH₂ PNP), 30.90 (t, $J_{\text{CP}} = 11.4$ Hz, CH *i*Pr), 30.55 (CH₃ *t*Bu), 30.21 (CH₃ *t*Bu), 27.79 (t, $J_{\text{CP}} = 10.8$ Hz, CH₂ PNP), 26.63 (t, $J_{\text{CP}} = 9.6$ Hz, CH *i*Pr), 20.09 (CH₃ *i*Pr), 19.88 (CH₃ *i*Pr), 19.54 (CH₃ *i*Pr). 2D {¹⁵N-¹H} HSQC NMR (300 K, CD₂Cl₂, 40.565 MHz, ppm): δ 14.7 (NH PNP). 2D {¹⁵N-¹H} HMBC NMR (300 K, CD₂Cl₂, 40.565 MHz, ppm): δ 194.2 (CN-*t*Bu).

[RuH(BH₄)(CN-CH₂Ph)(PN^HP)] (3a). To the suspension of **1a** (0.5 g, 0.84 mmol) in EtOH (50 mL) was added NaBH₄ (0.160 g, 4.2 mmol) at RT. The reaction mixture was stirred at RT for 20 h. The resulting colorless solution was evaporated to dryness under reduced pressure. The residual white solids were extracted with toluene (2x30mL). The extracts were filtered and evaporated to dryness. Yield: 0.31 g, 67%. Anal. Calcd. for C₂₄H₄₉BN₂P₂Ru: C 53.43; H 9.16; N 5.19. Found C 54.13; H 9.43; N 5.19. ¹H NMR (298 K, C₆D₆, 400.33 MHz, ppm): δ 7.21-7.09 (m, 4H, C_{Ar}-H, Ph), 7.02 (t, 1H, $J_{\text{HH}} = 7.1$ Hz, *para*-C_{Ar}-H, Ph), 4.32 (s, 2H, CH₂Ph), 3.98 (br t, 1H, $J_{\text{HN}} = 11.1$ Hz, NH), 2.80 (m, 2H, CH *i*Pr), 2.54 (m, 2H, CH₂ PNP), 1.92 (m, 2H, CH *i*Pr), 1.82-1.56 (m, 6H, CH₂ PNP), 1.50 (dt, 6H, $J_{\text{HH}} = 7.4$ Hz, $J_{\text{HP}} = 7.5$ Hz, CH₃ *i*Pr), 1.13 (dt, 12H, $J_{\text{HH}} = 7.0$ Hz, $J_{\text{HP}} = 6.7$ Hz, CH₃ *i*Pr), 1.02 (dt, 6H, $J_{\text{HH}} = 6.9$ Hz, $J_{\text{HP}} = 6.9$ Hz, CH₃ *i*Pr), -1.50 (br d,

4H, BH₄), -14.33 (t, 1H, ²J_{HP} = 18.4 Hz, Ru-H). ³¹P{¹H} NMR (298 K, C₆D₆, 121.495 MHz, ppm): δ 77.57 (PNP). ¹³C{¹H} NMR (298 K, C₆D₆, 100.663 MHz, ppm): δ 137.19 (CH₂C_{Ar}), 128.79, 127.58, 127.17 (C_{Ar}-H), 54.56 (t, J_{CP} = 5.3 Hz, CH₂ PNP), 48.14 (CH₂Ph), 30.01 (t, 2C, J_{CP} = 8.3 Hz, CH₂ PNP), 29.02 (t, ¹J_{CP} = 10.2 Hz, CH *i*Pr), 24.46 (t, ¹J_{CP} = 11.7 Hz, CH *i*Pr), 21.31 (t, ²J_{CP} = 3.6 Hz, CH₃ *i*Pr), 20.82 (t, ²J_{CP} = 3.6 Hz, CH₃ *i*Pr), 19.1 (CH₃ *i*Pr), 18.08 (CH₃ *i*Pr). 2D {¹⁵N-¹H} HSQC NMR (293 K, C₆D₆, 40.565 MHz, ppm): δ 47.3 (NH). 2D {¹⁵N-¹H} HMBC NMR (293 K, C₆D₆, 40.565 MHz, ppm): δ 160.04 (CNCH₂Ph). ¹¹B{¹H} NMR (293 K, C₆D₆, 128.442 MHz, ppm): δ -33.46 (br, BH₄).

[RuH(BH₄)(CN-*n*Bu)(PN^HP)] (3b). The complex was prepared in a similar manner to the procedure described above for **3a**. Yield: 69%. Anal. Calcd. for C₂₁H₅₁BN₂P₂Ru: C 49.90; H 10.17; N 5.54. Found: C 50.04; H 10.26; N 5.68. ¹H NMR (298 K, C₇D₈, 400.33 MHz, ppm): δ 3.92 (br, 1H, NH), 3.07 (t, 2H, ³J_{HH} = 6.5 Hz, CN-CH₂), 2.72 (m, 2H, CH *i*Pr), 2.61 (m, 2H, CH₂ PNP), 1.95 (m, 2H, CH *i*Pr), 1.8-1.57 (m, 6H, CH₂ PNP), 1.50 (dt, 6H, J_{HH} = 7.4 Hz, J_{HP} = 7.5 Hz, CH₃ *i*Pr), 1.21 (m, 2H, CH₂ *n*Bu), 1.19-1.1 (m, 14H, 2H, CH₂ *n*Bu and 12H, CH₃ *i*Pr), 1.02 (dt, 6H, J_{HH} = 6.9 Hz, J_{HP} = 6.9 Hz, CH₃ *i*Pr), 0.74 (t, 3H, ³J_{HH} = 7.1 Hz, CH₃ *n*Bu), -1.80 (br, 4H, BH₄), -14.67 (t, 1H, ²J_{HP} = 18.8 Hz, Ru-H). ³¹P{¹H} NMR (298 K, C₇D₈, 121.495 MHz, ppm): δ 77.73 (PNP). ¹³C{¹H} NMR (298 K, C₇D₈, 75.468 MHz, ppm): δ 176.68 (t, ²J_{CP} = 12.8 Hz, CN-*n*Bu), 54.2 (t, J_{CP} = 4.3 Hz, CH₂ PNP), 43.57 (CN-CH₂), 32.63 (CH₂ *n*Bu), 29.94 (t, J_{CP} = 8.4 Hz, CH₂ PNP), 28.90 (t, J_{CP} = 10 Hz, CH *i*Pr), 24.5 (t, J_{CP} = 11.5 Hz, CH *i*Pr), 21.15 (CH₃ *i*Pr), 20.59 (CH₃ *i*Pr), 19.87 (CH₂ *n*Bu), 18.94 (CH₃ *i*Pr), 17.92 (CH₃ *i*Pr), 13.33 (CH₃ *n*Bu). 2D {¹⁵N-¹H} HSQC NMR (293 K, C₇D₈, 40.565 MHz, ppm): δ 44.6 (NH, PNP). 2D {¹⁵N-¹H} HMBC NMR (298 K, C₇D₈, 40.565 MHz, ppm): δ 163.02 (CN-*n*Bu). ¹¹B{¹H} NMR (298 K, C₇D₈, 128.442 MHz, ppm): δ -33.99 (br, BH₄).

[RuH(BH₄)(CN-*t*Bu)(PN^HP)] (3c). The complex was prepared in a similar manner to the procedure described above for **3a**. Yield: 73%. Anal. Calcd. for C₂₁H₅₁BN₂P₂Ru: C 49.90; H 10.17; N 5.54. Found: C 50.02; H 10.07; N 5.60. FT-IR (ν, cm⁻¹): 3206.9 (w, NH), 2371, 2327.4 (vs), 2298 (Ru-HBH₃), 2024.2 (vs, Ru-CN), 1837.2 (m, Ru-H). ¹H NMR (298 K, C₇D₈, 400.33 MHz, ppm): δ 3.89 (br, 1H, NH), 2.75 (m, 2H, CH *i*Pr), 2.51 (m, 2H, CH₂ PNP), 1.97 (m, 2H, CH *i*Pr), 1.72-1.56 (m, 6H, CH₂ PNP), 1.52 (dt, 6H, J_{HH} = 7.4 Hz, J_{HP} = 7.5 Hz, CH₃ *i*Pr), 1.15 (dt, 12H, J_{HH} = 7.0 Hz, J_{HP} = 6.5 Hz, CH₃ *i*Pr), 1.09 (s, 9H, CH₃ *t*Bu), 1.02 (dt, J_{HH} = 6.8 Hz, J_{HP} = 6.8 Hz, 6H, CH₃ *i*Pr), -1.31 (br, 4H, BH₄), -14.78 (t, ²J_{HP} = 18.6 Hz, 1H, Ru-H). ³¹P{¹H} NMR (298 K, C₇D₈, 121.495 MHz, ppm): δ 77.32 (PNP). ¹³C{¹H-³¹P} NMR (298 K, C₇D₈, 100.663 MHz, ppm): δ 169 (CN-*t*Bu), 54.7 (C_{quat}. *t*Bu), 54.4 (CH₂ PNP), 31.0 (CH₃ *t*Bu), 30.1 (CH₂ PNP), 29.4 (CH *i*Pr), 24.9 (CH *i*Pr), 21.4 (CH₃ *i*Pr), 20.7 (CH₃ *i*Pr), 19.1 (CH₃ *i*Pr), 17.9 (CH₃ *i*Pr). 2D {¹H-¹³C} HMBC NMR (298 K, C₇D₈,

100.663 MHz, ppm): 169 (CN-*t*Bu). 2D $\{^{15}\text{N}-^1\text{H}\}$ HSQC NMR (298 K, C_7D_8 , 40.565 MHz, ppm): δ 47.0 (NH). 2D $\{^{15}\text{N}-^1\text{H}\}$ HMBC NMR (298 K, C_7D_8 , 40.565 MHz, ppm): δ 184.61 (CN-*t*Bu). $^{11}\text{B}\{^1\text{H}\}$ NMR (298 K, C_7D_8 , 128.4418 MHz, ppm): δ -33.86 (br, 1B, BH_4).

[RuHCl(CN-CH₂Ph)(PN^HP)] (4a). To the suspension of **1a** (0.4g, 0.67mmol) in EtOH (40mL) was slowly added the solution of NaBH₄ (1 equiv., 0.026g) in EtOH (10mL) at 0 °C. The reaction mixture was stirred at RT for 20h. The resulting colorless solution was evaporated to dryness under reduced pressure. The residual white solids were extracted with toluene and the solution was filtered and concentrated. The crystallization process was performed by addition of *n*-pentane while maintaining the solution at -20 °C. After 20h, white crystals formed and were collected and washed with *n*-pentane (3x5mL) and dried under vacuum. Yield: 0.22g, 59%. Anal. Calcd. for C₂₄H₄₅ClN₂P₂Ru: C 51.47; H 8.10; N 5.00. Found: C 51.48; H 8.26; N 5.06. ^1H NMR (298 K, C_6D_6 , 400.33 MHz, ppm): δ 7.33 (d, 2H, $^3J_{\text{HH}} = 7.5$ Hz, *ortho*-C_{Ar}-H), 7.17 (t, 2H, $^3J_{\text{HH}} = 8.0$ Hz, *meta*-C_{Ar}-H), 7.05 (t, 1H, $^3J_{\text{HH}} = 7.3$ Hz, *para*-C_{Ar}-H, Ph), 4.52 (s, 2H, CH₂Ph), 3.55 (br t, 1H, $^3J_{\text{HH}} = 12.0$ Hz, NH), 3.02 (m, 2H, CH *i*Pr), 2.58 (m, 2H, CH₂ PNP), 1.94 (m, 2H, $J_{\text{HH}} = 6.8$ Hz, CH *i*Pr), 1.81 (m, 2H, CH₂ PNP), 1.71-1.50 (m, 4H, CH₂ PNP), 1.62 (dt, 6H, $J_{\text{HH}} = 7.4$ Hz, $J_{\text{HP}} = 7.6$ Hz, CH₃ *i*Pr), 1.19 (dt, 6H, $J_{\text{HH}} = 6.4$ Hz, $J_{\text{HP}} = 7.8$ Hz, CH₃ *i*Pr), 1.17 (dt, $J_{\text{HH}} = 6.4$ Hz, $J_{\text{HP}} = 5.6$ Hz, 6H, CH₃ *i*Pr), 1.02 (dt, 6H, $J_{\text{HH}} = 7.0$ Hz, $J_{\text{HP}} = 6.9$ Hz, CH₃ *i*Pr), -17.10 (t, 1H, $^2J_{\text{HP}} = 18.7$ Hz, Ru-H). $^{31}\text{P}\{^1\text{H}\}$ NMR (298 K, C_6D_6 , 121.495 MHz, ppm): δ 74.21 (PNP). $^{13}\text{C}\{^1\text{H}\}$ NMR (298 K, C_6D_6 , 100.663 MHz, ppm): δ 128.61 (C_{Ar}-H), 127.27 (C_{Ar}-H), 127.14 (C_{Ar}-H), 53.98 (t, $^2J_{\text{CP}} = 4.8$ Hz, CH₂ PNP), 48.36 (CH₂Ph), 30.43 (t, $J_{\text{CP}} = 7.9$ Hz, CH₂ PNP), 26.81 (t, $^1J_{\text{CP}} = 9.6$ Hz, CH *i*Pr), 24.27 (t, $^1J_{\text{CP}} = 11.4$ Hz, CH *i*Pr), 21.33 (t, $^2J_{\text{CP}} = 2.7$ Hz, CH₃ *i*Pr), 20.96 (t, $^2J_{\text{CP}} = 3.7$ Hz, CH₃ *i*Pr), 19.23 (CH₃ *i*Pr), 17.78 (CH₃ *i*Pr). 2D $\{^{15}\text{N}-^1\text{H}\}$ HSQC NMR (293 K, C_6D_6 , 40.565 MHz, ppm): δ 55.1 (NH). 2D $\{^{15}\text{N}-^1\text{H}\}$ HMBC NMR (293 K, C_6D_6 , 40.565 MHz, ppm): δ 160.04 (CNCH₂Ph).

[RuHCl(CN-*n*Bu)(PN^HP)] (4b). Complex **4b** was prepared in a similar manner as described for the synthesis of **4a**, starting from **1b**. Yield: 55%. Anal. Calcd. for C₂₁H₄₇ClN₂P₂Ru: C 47.95; H 9.01; N 5.33. Found: 47.40, H 9.72, N 4.95. FT-IR (v, cm⁻¹): 3170.1 (m, ν_{NH}), 2075, 2056 (vs, $\nu_{\text{C}\equiv\text{N}}$), 1949.3 (s, ν_{RuH}). ^1H NMR (293 K, C_6D_6 , 400.33 MHz, ppm): δ 3.79 (br t, 1H, $^3J_{\text{HH}} = 11.9$ Hz, NH), 3.23 (t, 2H, $^3J_{\text{HH}} = 6.1$ Hz, CNCH₂(CH₂)₂CH₃), 3.04 (m, 2H, CH *i*Pr), 2.79 (br m, 2H, CH₂ PNP), 2.0 (m, 2H, CH *i*Pr), 1.89-1.58 (m, 6H, CH₂ PNP), 1.68 (td, 6H, $^3J_{\text{HH}} = 7.5$ Hz, $^3J_{\text{HP}} = 7.5$ Hz, CH₃ *i*Pr), 1.36-1.19 (m, 4H, CNCH₂(CH₂)₂CH₃), 1.24 (m, 12H, CH₃ *i*Pr), 1.05 (td, 6H, $^3J_{\text{HH}} = 7.0$ Hz, $^3J_{\text{HP}} = 7.1$ Hz, CH₃ *i*Pr), 0.75 (t, 3H, $^3J_{\text{HH}} = 7.1$ Hz, CNCH₂(CH₂)₂CH₃), -17.58 (t, 1H, $^2J_{\text{HP}} = 18.9$ Hz, Ru-H). $^{31}\text{P}\{^1\text{H}\}$ NMR (298 K, C_6D_6 , 121.495 MHz, ppm): δ 74.54 (PNP). $^{13}\text{C}\{^1\text{H}\}$ NMR (298 K, C_6D_6 , 100.663 MHz, ppm): δ 182.37 (t, $^1J_{\text{CP}} = 11.9$ Hz, CN(CH₂)₃CH₃),

54.49 (t, $J_{CP} = 5.8$ Hz, CH₂ PNP), 44.33 (CNCH₂(CH₂)₂CH₃), 33.40 (CNCH₂CH₂CH₂CH₃), 30.93 (t, $J_{CP} = 7.4$ Hz, CH₂ PNP), 27.25 (t, $^1J_{CP} = 9.2$ Hz, CH *iPr*), 24.8 (t, $^1J_{CP} = 11.8$ Hz, CH *iPr*), 21.75 (t, $^2J_{CP} = 3$ Hz, CH₃ *iPr*), 21.31 (t, $^2J_{CP} = 3$ Hz, CH₃ *iPr*), 20.50 (CN(CH₂)₂CH₂CH₃), 19.63 (CH₃ *iPr*), 18.24 (CH₃ *iPr*), 13.94 (CN(CH₂)₃CH₃). 2D {¹⁵N-¹H} HSQC NMR (298 K, C₆D₆, 40.565 MHz, ppm): δ 53.8 (NH). 2D {¹⁵N-¹H} HMBC NMR (298 K, C₆D₆, 40.565 MHz, ppm): δ 162.5 (CN-*n*Bu).

[RuHCl(CN-*t*Bu)(PN^HP)] (4c). Complex **4c** was prepared in a similar manner as described for the synthesis of **4a**, starting from **1c**. Yield: 62%. Anal. Calcd. for C₂₁H₅₁BN₂P₂Ru: C 47.95; H 9.01; N 5.33. Found: C 47.37, H 9.75, N 5.14. ¹H NMR (298 K, C₇D₈, 400.33 MHz, ppm): δ 3.73 (br t, 1H, $J_{HN} = 11.7$ Hz, NH), 3.05 (m, 2H, CH *iPr*), 2.73 (m, 2H, CH₂ PNP), 2.02 (m, 2H, CH *iPr*), 1.90-1.50 (m, 6H, CH₂ PNP), 1.69 (dt, 6H, $^3J_{HH} = 7.2$ Hz, $^3J_{HP} = 7.4$ Hz, CH₃ *iPr*), 1.25 (m, 6H, CH₃ *iPr*), 1.24 (m, 6H, CH₃ *iPr*), 1.18 (s, 9H, CH₃ *t*Bu), 1.05 (dt, 6H, $^3J_{HH} = 6.8$ Hz, $^3J_{HP} = 6.9$ Hz, CH₃ *iPr*), -17.8 (t, 1H, $^2J_{HP} = 18.8$ Hz, Ru-H). ³¹P{¹H} NMR (298 K, C₇D₈, 121.495 MHz, ppm): δ 74.0 (PNP). ¹³C{¹H} NMR (298 K, C₇D₈, 100.663 MHz, ppm): δ 174.0 (CN-*t*Bu), 54.59 (C quat. *t*Bu), 54.22 (t, $J_{CP} = 5.0$ Hz, CH₂ PNP), 31.51 (CH₃ *t*Bu), 30.72 (t, $J_{CP} = 8.2$ Hz, CH₂ PNP), 27.36 (t, $^1J_{CP} = 10.2$ Hz, CH *iPr*), 24.80 (t, $^1J_{CP} = 10.9$ Hz, CH *iPr*), 21.63 (t, $^2J_{CP} = 2.9$ Hz, CH₃ *iPr*), 21.09 (t, $^2J_{CP} = 4.3$ Hz, CH₃ *iPr*), 19.28 (CH₃ *iPr*), 17.87 (CH₃ *iPr*). 2D {¹⁵N-¹H} HSQC NMR (298 K, C₇D₈, 40.565 MHz, ppm): δ 54.0 (NH). 2D {¹⁵N-¹H} HMBC NMR (298 K, C₇D₈, 40.565 MHz, ppm): δ 184.23 (CN-*t*Bu).

Characterization of [RuH₂(CN-CH₂Ph)(PN^HP)] (5a). To the suspension of **1a** (0.3g, 0.51 mmol) in toluene (10 mL) was added a solution of NaHBET₃ in toluene (1M, 2.1 equiv., 1.06 mmol) at -18 °C. The reaction mixture was stirred at room temperature. After 14 h, the yellow solution was filtered through-out a celite column and evaporated under vacuum to afford a yellow solid. Attempts to purify the product were unsuccessful due to its low stability. Selected characterization elements: ¹H NMR (300 K, C₆D₆, 300.129MHz, ppm): δ 4.45 (s, 2H, CH₂Ph), -6.25 (td, 1H, $^2J_{HH} = 6.8$ Hz, $^2J_{HP} = 18.4$ Hz, Ru-H), -6.48 (td, 1H, $^2J_{HH} = 6.9$ Hz, $^2J_{HP} = 19$ Hz, Ru-H). ³¹P{¹H} NMR (300 K, C₆D₆, 121.495 MHz, ppm): δ 86.89 (PNP).

[RuH₂(CN-*t*Bu)(PN^HP)] (5c). To a suspension of **1c** (0.34g, 0.61 mmol) in toluene (10 mL) was slowly added a solution of NaHBET₃ in toluene (2.1 equiv., 1M, 1.28 mmol) at -18 °C. The reaction mixture was stirred for 14 h at room temperature. The resulting yellow solution was filtered throughout a celite column. The obtained solution was concentrated under reduced pressure and *n*-pentane was poured. Slow crystallization at -18 °C afford **5c**. Yield: 0.185g, 62%. As described above, two *fac/mer* isomers were obtained in respective ratio of 1/1.5. No satisfactory results were obtained due to

complex decomposition. For *fac*-isomer **fac-5c**: Selected data: ^1H NMR (285 K, C_7D_8 , 400.33 MHz, ppm): δ 3.84 (br, 1H, NH), 1.14 (s, 9H, CH_3 CN-*t*Bu), -8.82 (m, 2H, Ru-H). $^{31}\text{P}\{^1\text{H}\}$ NMR (285 K, C_7D_8 , 121.495 MHz, ppm): δ 74.08 (PNP). 2D $\{^{15}\text{N}-^1\text{H}\}$ HSQC (285 K, C_7D_8 , 40.565 MHz, ppm): δ 19.45 (PNP). 2D $\{^{15}\text{N}-^1\text{H}\}$ HMBC (255K, C_7D_8 , 40.565 MHz, ppm): δ 178 (CN-*t*Bu). For *mer*-isomer **mer-5c**: Selected data ^1H NMR (285 K, C_7D_8 , 400.33 MHz, ppm): δ 2.48 (br, 1H, NH), 1.16 (s, 9H, CH_3 CN-*t*Bu), -6.86 (td, 1H, $^2J_{\text{HH}} = 4.9$ Hz, $^2J_{\text{HP}} = 18$ Hz, Ru-H), -7.05 (td, 1H, $J_{\text{HH}} = 4.0$ Hz, $^2J_{\text{HP}} = 19$ Hz, Ru-H). $^{31}\text{P}\{^1\text{H}\}$ NMR (285 K, C_7D_8 , 121.495 MHz, ppm): δ 84.78 (s, PNP). 2D $\{^{15}\text{N}-^1\text{H}\}$ HSQC (285 K, C_7D_8 , 40.565 MHz, ppm): δ 31.0 (PNP). 2D $\{^{15}\text{N}-^1\text{H}\}$ HMBC (255 K, C_7D_8 , 40.565 MHz, ppm): δ 184.6 (CN-*t*Bu). Isomeric mixture $^{13}\text{C}\{^1\text{H}\}$ NMR (285 K, C_7D_8 , 100.663 MHz, ppm): δ 54.12 (CH_2 PNP), 52.35 (CH_2 PNP), 32.90 (CH *i*Pr), 31.70 (CH_3 CN-*t*Bu), 31.59 (CH_3 CN-*t*Bu), 30.48 (CH *i*Pr), 28.42 (CH_2 PNP), 27.13 (CH_2 PNP), 27.11 (CH *i*Pr), 26.43 (CH *i*Pr), 22.33 (CH_3 *i*Pr), 20.46 (CH_3 *i*Pr), 20.01 (CH_3 *i*Pr), 19.99 (CH_3 *i*Pr), 18.3 (CH_3 *i*Pr).

[RuH(CN-*t*Bu)(PNP)] (6). To a solution of **4c** (30 mg, 0.057 mmol) in deuterated benzene (1 mL) was added *t*BuOK (1.02 eq., 0.058 mmol) at $^\circ\text{C}$. After stirring for 14h at RT, the yellow reaction mixture was filtered and analyzed by NMR. Selected characterization data: ^1H NMR (300 K, C_6D_6 , 300.129 MHz, ppm): δ -18.74 (t, 1H, $^2J_{\text{HP}} = 16.5$ Hz, Ru-H). $^{31}\text{P}\{^1\text{H}\}$ NMR (300 K, C_6D_6 , 121.495 MHz, ppm): δ 91.78 (PNP).

[RuH(CN- CH_2Ph) $_2$ (PN $^{\text{H}}$ P)]Cl (7). To a solution of **1a** (0.15 g, 0.268 mmol) in toluene (6 mL) was slowly added a solution of benzylisocyanide (2.2 equiv., 69 mg) in toluene (1 mL) at RT. After stirring at RT for 24h, the resulting solution was evaporated to dryness under reduced pressure. The product was washed with *n*-pentane (3x3 mL). The product can be also purified by slow crystallization into toluene/*n*-pentane mixture at -18 $^\circ\text{C}$. After a few days, the white crystals were collected and washed with *n*-pentane (5mLx3) and finally dried under vacuum. Yield: 0.12 g, 67%. Anal. Calcd. for $\text{C}_{32}\text{H}_{52}\text{ClN}_3\text{P}_2\text{Ru}$: C 56.75; H 7.74; N 6.21. Found: 57.03, H 8.01, N 5.98. FT-IR (ν , cm^{-1}): 3055 (s, ν_{NH}), 2135.2 (vs), 2059.3 (vs, $\nu_{\text{C}\equiv\text{N}}$), 1816 (m, $\nu_{\text{Ru-H}}$). ^1H NMR (293 K, C_6D_6 , 400.33 MHz, ppm): δ 8.43 (br t, $^3J_{\text{HN}} = 10.2$ Hz, 1H, NH), 7.78 (d, $^3J_{\text{HH}} = 7.7$ Hz, 2H, *ortho*- C_{Ar} -H), 7.20-7.12 (m, 2H, C_{Ar} -H), 7.12-7.01 (m, 4H, C_{Ar} -H), 7.0-6.96 (m, 2H, C_{Ar} -H), 5.31 (s, 2H, CH_2Ph), 4.05 (s, 2H, CH_2Ph), 3.35 (m, 2H, CH_2 PNP), 2.31 (m, 2H, CH_2 PNP), 1.97 (m, 2H, CH *i*Pr), 1.85 (m, 2H, CH *i*Pr), 1.79-1.67 (m, 4H, CH_2 PNP), 1.21 (dt, 6H, $^3J_{\text{HH}} = 7.4$ Hz, $^3J_{\text{HP}} = 7.5$ Hz, CH_3 *i*Pr), 1.02 (m, 6H, CH_3 *i*Pr), 1.01 (m, 6H, CH_3 *i*Pr), 0.98 (m, 6H, CH_3 *i*Pr) -8.48 (t, $^2J_{\text{HP}} = 18.9$ Hz, 1H, Ru-H). $^{31}\text{P}\{^1\text{H}\}$ NMR (298 K, C_6D_6 , 121.495 MHz, ppm): δ 78.86 (PNP). $^{13}\text{C}\{^1\text{H}\}$ NMR (298 K, C_6D_6 , 100.663 MHz, ppm): δ 171.38 (t, $^2J_{\text{CP}} = 11.0$ Hz, CN CH_2Ph), 157.42 (t, $^2J_{\text{CP}} = 8.4$ Hz, CN CH_2Ph), 135.50, 135.29

(CH₂C_{Ar}), 129.67, 129.34, 128.75, 127.95, 127.07, 125.70 (C_{Ar}-H, Ph), 55.22 (t, $J_{CP} = 3.7$ Hz, CH₂ PNP), 49.42, 47.78 (CH₂Ph), 31.02 (t, $^1J_{CP} = 11.4$ Hz, CH *i*Pr), 30.81 (t, $J_{CP} = 10.4$ Hz, CH₂ PNP), 24.63 (t, $^1J_{CP} = 12.3$ Hz, CH *i*Pr), 20.53 (t, $^2J_{CP} = 2.5$ Hz, CH₃ *i*Pr), 18.79 (t, $^2J_{CP} = 1.5$ Hz, CH₃ *i*Pr), 18.27 (CH₃ *i*Pr). 2D {¹⁵N-¹H} HSQC NMR (293 K, C₆D₆, 40.565 MHz, ppm): δ 35.3 (NH). 2D {¹⁵N-¹H} HMBC NMR (293 K, C₆D₆, 40.565 MHz, ppm): δ 172.8, 159.4 (CNCH₂Ph).

[FeBr(CN-CH₂Ph)₂(PN^HP)]Br (8). To a white suspension of [FeBr₂(PNP^H)] (0.5 g, 0.96 mmol) in toluene (30 mL) was added dropwise a solution of benzyl isocyanide (3.0 equiv., 2.88 mmol, 0.337 g) in toluene (10 mL) at room temperature. The reaction mixture immediately turned out to green. After stirring for 20h at RT, the green-lemon solution was concentrated under reduced pressure and *n*-pentane (30 mL) was added. After overnight storage at -20 °C, a green precipitate was obtained, washed with *n*-pentane (4 x 20 mL) and dried under vacuum. Yield: 0.59 g, 82%. Anal. Calcd. for C₃₂H₅₁Br₂N₃P₂Fe: C 50.88; H 6.81; N 5.56. Found: C 50.98, H 6.91, N 5.23. FT-IR (cm⁻¹): 3060.9 (m, ν_{NH}), 2148.6, 2114.2 (s, ν_{C≡N}). Major isomer (**cis-8/trans-8** ratio: 15.6/1): ¹H NMR (293 K, CD₂Cl₂, 800.13 MHz, ppm): δ 7.49 (m, 2H, C_{Ar}-H), 7.4-7.33 (m, 6H, C_{Ar}-H), 7.30 (m, 2H, C_{Ar}-H), 6.51 (br t, $^3J_{HH} = 11.1$ Hz, 1H, NH), 5.06 (s, 2H, CNCH₂Ph), 4.80 (s, 2H, CNCH₂Ph), 3.04 (m, 2H, CH₂ PNP), 2.99 (m, 2H, CH *i*Pr), 2.76 (m, 2H, CH₂ PNP), 2.26 (m, 2H, CH₂ PNP), 2.17 (m, CH₂ PNP), 2.14 (m, 2H, CH *i*Pr), 1.37 (m, 6H, CH₃ *i*Pr), 1.36 (m, 6H, CH₃ *i*Pr), 1.18 (td, $^3J_{HH} = 7.2$ Hz, $^3J_{HP} = 7.0$ Hz, 6H, CH₃ *i*Pr), 1.05 (td, 6H, $^3J_{HH} = 7.4$ Hz, $^3J_{HP} = 7.5$ Hz, CH₃ *i*Pr). ¹³C{¹H} NMR (298 K, CD₂Cl₂, 100.663 MHz, ppm): δ 171.1, 166.2 (CNCH₂Ph), 133.44, 133.19 (CH₂C_{Ar}), 129.32, 129.23, 127.9 (C_{Ar}-H), 51.2, 49.6 (CNCH₂Ph), 49.6 (CH₂ PNP), 29.44 (t, $^1J_{CP} = 11$ Hz, CH *i*Pr), 27.67 (t, $J_{CP} = 8.3$ Hz, CH₂ PNP), 24.67 (t, $^1J_{CP} = 8.4$ Hz, CH *i*Pr), 20.01, 19.73, 19.65, 19.38 (CH₃ *i*Pr). ³¹P{¹H} NMR (298 K, CD₂Cl₂, 121.495 MHz, ppm): δ 72.0 (PNP). 2D {¹⁵N-¹H} HSQC NMR (298 K, CD₂Cl₂, 40.565 MHz, ppm): δ 30.2 (NH). 2D {¹⁵N-¹H} HMBC NMR (298 K, CD₂Cl₂, 40.565 MHz, ppm): δ 188.7, 183.5 (CNCH₂Ph). Minor isomer **trans-8**: ¹H NMR (298 K, CD₂Cl₂, 800.13 MHz, ppm): δ 7.76 (m, 2H, C_{Ar}-H), 7.48 (m, 2H, C_{Ar}-H), 7.45-7.33 (m, 6H, C_{Ar}-H), 5.44, 5.16 (s, 2H, CNCH₂Ph), 4.02 (br t, $^3J_{HH} = 11.4$ Hz, 1H, NH, PNP), 2.69, 2.60 (m, 2H, CH *i*Pr), 2.76 (m, 2H, CH₂ PNP), 2.43 (m, 2H, CH₂ PNP), 1.97 (m, 2H, CH₂ PNP), 1.69 (m, 2H, CH₂ PNP), 1.44, 1.35, 1.34 (m, 6H, CH₃ *i*Pr), 1.30 (m, 2H, CH₂ PNP), 1.22 (m, 6H, CH₃ *i*Pr). ¹³C{¹H} NMR (298 K, CD₂Cl₂, 100.663 MHz, ppm): δ 174, 168 (CNCH₂Ph), 133.3, 133.1 (C_{Ar} quat.), 129.3, 128.2 (C_{Ar}-H), 52.9 (CH₂ PNP), 50.3, 50.0 (CNCH₂Ph), 29.4 (CH *i*Pr), 27.6 (CH₂ PNP), 24.7 (t, CH *i*Pr), 20.5, 20.0, 19.8, 19.7 (CH₃ *i*Pr). ³¹P{¹H} NMR (298 K, CD₂Cl₂, 121.495 MHz, ppm): δ 58.0 (PNP). 2D {¹⁵N-¹H} HMBC NMR (298 K, CD₂Cl₂, 40.565 MHz, ppm): δ 186.3, 183.2 (CNCH₂Ph).

[FeBr(CN-CH₂Ph)₂(PN^HP)](BPh₄) (9). To a lemon-green solution of [FeBr(CN-CH₂Ph)₂(PN^HP)]Br (**8**) (0.31 g, 0.40 mmol) in toluene (20 mL) was added NaBPh₄ in excess (0.68 g, 5 equiv., 2.0 mmol) at room temperature. The reaction mixture was stirred at room temperature for 20 h, and filtered throughout a celite column. The obtained solution was evaporated to dryness. The residual solid was dissolved in a minimum volume of CH₂Cl₂ (2 mL) and *n*-pentane (8 mL) was poured. Slow crystallization at -18 °C afforded **9**. Yield: 0.21g, 53%. Crystals suitable for X-ray analysis were obtained similarly. FT-IR (cm⁻¹): 3227 (s, ν_{NH}), 2146 (s), 2108 (s, ν_{C≡N}). ¹H NMR (300 K, CD₂Cl₂, 300.13 MHz, ppm): δ 7.5 -7.3 (14H, C_{Ar}-H), 7.3-7.18 (4H, C_{Ar}-H), 7.03 (t, ³J_{HH} = 7.4 Hz, 8H, C_{Ar}-H), 6.88 (m, 4H, C_{Ar}-H), 4.76, 4.63 (s, 2H, CNCH₂Ph), 2.99 (m, 2H, CH *i*Pr), 2.78-2.53 (m, 4H, CH₂ PNP), 2.40 (t, ³J_{HH} = 11.8 Hz, 1H, NH), 2.2 (m, 2H, CH₂ PNP), 2.05 (m, 2H, CH *i*Pr), 1.37 (dt, ³J_{HH} = 7.3 Hz, ³J_{HP} = 7.3 Hz, 6H, CH₃, *i*Pr), 1.34 (dt, ³J_{HH} = 7.5 Hz, ³J_{HP} = 7.5 Hz, 6H, CH₃ *i*Pr), 1.27 (m, 2H, CH₂ PNP), 1.21 (dt, ³J_{HH} = 6.8 Hz, ³J_{HP} = 6.1 Hz, 6H, CH₃ *i*Pr), 1.09 (dt, ³J_{HH} = 7.4 Hz, ³J_{HP} = 7.7 Hz, 6H, CH₃ *i*Pr). ¹³C{¹H} NMR (298 K, CD₂Cl₂, 75.468 MHz, ppm): δ 164.52 (q, ¹J_{CB} = 50.1 Hz, C_{Ar} quart. BPh₄), 136.58 (s, C_{Ar}-H), 132.54 (C_{Ar} quat.), 130.06, 130.02, 129.66, 129.49, 128.59, 128.34, 126.16, 122.31 (C_{Ar}-H), 50.89, 49.92 (CN-CH₂), 49.63 (t, J_{CP} = 3.2 Hz, CH₂ PNP), 29.87 (t, ¹J_{CP} = 11 Hz, CH *i*Pr), 28.23 (t, J_{CP} = 8.5 Hz, CH₂ PNP), 25.00 (t, ¹J_{CP} = 9.2 Hz, CH *i*Pr), 20.03, 19.72, 19.56, 19.42 (CH₃, *i*Pr).

[FeH(CN-*t*Bu)₂(PN^HP)](BH₄) (10). To a suspension of [FeBr₂(PN^HP)] (0.3g, 0.58mmol) in toluene (30 mL) was added a solution of *t*-butylisocyanide (3 equiv.; 1.73 mmol, 0.144g) in toluene (2mL) at room temperature. After stirring for 20h and evacuation to dryness, ethanol (30 mL) was added, affording a yellow suspension. After cooling at -18 °C, a solution of excess NaBH₄ (10 molar equiv.) in ethanol (10 mL). The reaction mixture was allowed to warm up to room temperature, stirred for 16h then evaporated to dryness under reduced pressure. Extraction with toluene (3 x 5mL) was performed and the combined extracts were concentrated. Addition of *n*-pentane at -18 °C afforded a microcrystalline white solid. Yield: 0.154g, (49%. Anal. Calcd. for C₂₆H₆₀BFen₃P₂: C 57.47; H 11.13; N 7.73. Found: C 58.29; H 12.21; N 7.91. FT-IR (cm⁻¹): 3058.1 (s, NH), 2284, 2210 (w, BH₄), 2111.1 (s), 2046.9 (vs, CN). ¹H NMR (293 K, C₆D₆, 400.33 MHz, ppm): δ 6.29 (br, 1H, NH), 3.28 (m, 2H, CH₂ PNP), 2.32 (m, 2H, CH *i*PrP), 2.09 (m, 2H, CH₂ PNP), 2.02 (m, 2H, CH *i*PrP), 1.60 (br m, 2H, CH₂ PNP), 1.56 (s, 9H, CH₃ *t*Bu), 1.41 (br m, 2H, CH₂ PNP), 1.33 (td, ³J_{HH} = 7.4 Hz, ³J_{HP} = 7.3 Hz, 6H, CH₃ *i*PrP), 1.15 (td, ³J_{HH} = 7.1 Hz, ³J_{HP} = 6.9 Hz, CH₃ *i*Pr), 1.04 (m, J_{HH} = 7.0 Hz, J_{HP} = 6.8 Hz, 6H, CH₃ *i*Pr), 1.02 (m, ³J_{HH} = 7.1 Hz, ³J_{HP} = 6.7 Hz, CH₃ *i*Pr), 0.88 (s, 9H, CH₃ *t*Bu), -10.48 (t, ¹J_{HP} = 50 Hz, 1H, Ru]-H). ¹³C{¹H} NMR (298 K, CD₂Cl₂, 100.663 MHz, ppm): δ 175.39,

166.21 (CNtBu), 56.36, 55.33 (C quat. tBu), 54.28 (t, $J_{CP} = 4.1$ Hz, CH₂ PNP), 31.63 (t, $^1J_{CP} = 8.9$ Hz, CH *i*Pr), 30.77, 30.63 (CH₃ tBu), 30.03 (t, $J_{CP} = 9.4$ Hz, CH₂ PNP), 25.81 (t, $^1J_{CP} = 12.5$ Hz, CH *i*Pr), 20.73, 19.07, 18.78 (CH₃ *i*Pr). $^{31}\text{P}\{^1\text{H}\}$ NMR (298 K, C₆D₆, 121.495 MHz, ppm): δ 100.01 (2P). 2D $\{^{15}\text{N}-^1\text{H}\}$ HSQC NMR (298 K, C₆D₆, 40.565 MHz, ppm): δ 31.67 (NH). 2D $\{^{15}\text{N}-^1\text{H}\}$ HMBC NMR (298 K, C₆D₆, 40.565 MHz, ppm): δ 196.5, 193.2 (CNtBu). $^{11}\text{B}\{^1\text{H}\}$ NMR (293 K, C₆D₆, 128.4418 MHz, ppm): δ -38.9 (BH₄).

Catalytic tests. TOF₀ determination: For acceptorless dehydrogenative coupling reactions of butanol, the initial turnover frequency (TOF₀) was determined by plotting turnover number as a function of time. TOF₀ was calculated from the slope of the linear regression performed on the initial linear part of the plot. Typical procedure for acceptorless dehydrogenative coupling of 1-butanol conducted in Schlenk tubes: In an argon filled glove-box, the selected complex (6.5 μmol ; 60 ppm) was weighed in a Schlenk tube containing a stirring bar. After connection to a Schlenk line, 1-butanol (10 mL; 8.10 g; 109 mmol) was added via a syringe under an argon stream. The Schlenk tube was then equipped with a condenser topped by an argon bubbler. The system was heated using an oil bath (130 °C) and stirred magnetically under an argon stream. Aliquots (ca. 0.1 mL) were periodically sampled to monitor the reaction progress over time. Aliquots were diluted with CDCl₃ and analyzed by ^1H NMR for determination of yield, turnover number and turnover frequency.

X-ray Structure Determination. A single crystal of each compound was mounted under inert perfluoropolyether wax on a Mitegen MicroLoopTM. Single-crystal X-rays measurements were performed at 100K under N₂ stream from a Cryostream 700 device (OxfordCryosystems). Data were collected using an Apex II CCD 4K Bruker diffractometer ($\lambda = 0.71073$ Å). The structures were solved using SHELXT³⁸ and refined by least-squares procedures on F^2 using SHELXL2014.³⁹ All Hydrogen atoms were placed in theoretical positions and refined riding on their parent atoms except for the hydride H attached to the Ru, B and N atoms which was located from difference Fourier maps and refined isotropically. ORTEP drawings were generated with ORTEP-3.⁴⁰ Crystallographic data have been deposited at the Cambridge Crystallographic Data Centre as Supplementary Publication Nos. CCDC 2006531-2006538. Copies of the data can be obtained free of charge on application to the Director, CCDC, 12 Union Road, Cambridge CB2 1EZ, U.K. (fax, (+44) 1223- 336-033; e-mail, deposit@ccdc.cam.ac.uk).

Supporting Information

Electronic Supplementary Information (ESI) available: NMR spectra and X-ray crystallographic data (CIF).

Conflicts of interest

There are no conflicts of interest to declare.

Acknowledgments

This work was performed in partnership with the SAS PIVERT, within the frame of the French Institute for the Energy Transition (Institut pour la Transition Énergétique (ITE) P.I.V.E.R.T. (www.institut-pivert.com) selected as an Investment for the Future (“Investissements d’Avenir”). This work was supported, as part of the Investments for the Future, by the French Government under the reference ANR-001-01. The authors also thank the CNRS and University of Lille for their financial support.

References

- ¹ a) J. R. Khusnutdinova and D. Milstein *Angew. Chem. Int. Ed.* 2015, **54**, 12236 – 12273.
- ² a) A. Corma, J. Navas and M. J. Sabater, *Chem. Rev.* 2018, **118**, 1410–1459; b) T. Irrgang and R. Kempe, *Chem. Rev.* 2019, **119**, 2524–2549.
- ³ B. L. Conley, M. K. Pennington-Boggio, E. Boz and T. J. Williams, *Chem. Rev.* 2010, **110**, 2294–2312.
- ⁴ R. Noyori, M. Yamakawa and S. Hashiguchi, *J. Org. Chem.* 2001, **66**, 7931–7944.
- ⁵ C. Gunanathan and D. Milstein, *Science* 2013, **341**, 249-260.
- ⁶ a) Ed. Morales-Morales D. *Pincer Compounds: Chemistry and Applications*; Elsevier Inc. **2018**; b) S. Werkmeister, J. Neumann, K. Junge and M. Beller, *Chem. Eur. J.* 2015, **21**, 12226–12250; c) L. Alig, M. Fritz and S. Schneider, *Chem. Rev.* 2019, **119**, 2681–2751; d) P. A. Chase, R. A. Gossage and Gerard van Koten, *Top. Organomet. Chem.* 2016, **54**, 1-16.
- ⁷ a) M. Nielsen, A. Kammer, D. Junge, H. Cozzula, S. S. Gladiali and M. Beller, *Angew. Chem. Int. Ed.* 2011, **50**, 9593-9597; b) M. Bertoli, A. Choualeb, A. J. Lough, B. Moore, D. Spasyuk and D. G. Gusev, *Organometallics* 2011, **30**, 3479-3482; c) S. Chakraborty, H. Dai, P. Bhattacharya, N. T. Fairweather, M. S. Gibson, J. A. Krause and H. Guan, *J. Am. Chem. Soc.* 2014, **136**, 7869–7872; d) S. Chakraborty, P. O. Lagaditis, M. Förster, E. A. Bielinski, N. Hazari, M. C. Holthausen, W. D. Jones and S. Schneider, *ACS Catal.* 2014, **4**, 3994–4003.

-
- ⁸ a) J. Zhang, G. Leitus, Y. Ben-David and D. Milstein, *J. Am. Chem. Soc.* 2005, **127**, 10840-10841; b) D. Spasyuk, S. Smith, and D. G. Gusev, *Angew. Chem. Int. Ed.* **2012**, *51*, 2772-2775; c) D. Spasyuk, C. Vicent and D. G. Gusev, *J. Am. Chem. Soc.* 2015, **137**, 3743-3746; d) L. V. A. Hale, T. Malakar, K.-N. T. Tseng, P. M. Zimmerman, A. Paul and N. K. Szymczak, *ACS Catal.* 2016, **6**, 4799–4813; e) Z. Cao, H. Qiao and F. Zeng *Organometallics* 2019, **38**, 797–804.
- ⁹ a) M. Gargir, Y. Ben-David, G. Leitus, Y. Diskin-Posner, L. J. W. Shimon and D. Milstein, *Organometallics* 2012, **31**, 6207–6214; b) D. Spasyuk, S. Smith and D. G. Gusev, *Angew. Chem. Int. Ed.* 2013, **52**, 2538-2542; c) P. Puylaert, R. van Heck, Y. Fan, A. Spannenberg, W. Baumann, M. Beller, J. Medlock, W. Bonrath, L. Lefort, S. Hinze and J. G. de Vries, *Chem. Eur. J.* 2017, **23**, 8473–8481; d) P.A. Dub, B. L. Scott and J. C. Gordon, *Organometallics* 2015, **34**, 4464–4479.
- ¹⁰ a) G. A. Filonenko, M. J. B. Aguila, E. N. Schulpen, R. van Putten, J. Wiecko, C. Müller, L. Lefort, E. J. M. Hensen and E. A. Pidko, *J. Am. Chem. Soc.* 2015, **137**, 7620-7623; b) L. Le, J. Liu, T. He, D. Kim, E. J. Lindley, T. N. Cervarich, J. C.; Malek, J. Pham, M. R. Buck and A. R. Chianese, *Organometallics* **2018**, *37*, 3286–3297; c) X. He, Y. Li, H. Fu, X. Zheng, H. Chen, R. Li and X. Yu, *Organometallics*, 2019, **38**, 1750–1760.
- ¹¹ E. Fogler, M. A. Iron, J. Zhang, Y. Ben-David, Y. Diskin-Posner, G. Leitus, L. J. W. Shimon and D. Milstein *Inorg. Chem.* 2013, **52**, 11469–11479.
- ¹² O. Ogata, Y. Nakayama, H. Nara, M. Fujiwhara and Y. Kayaki, *Org. Lett.* 2016, **18**, 3894–3897.
- ¹³ a) N. E. Smith, W. H. Bernskoetter, N. Hazari and B. Q. Mercado, *Organometallics*, 2017, **36**, 3995–4004; b) J. B. Curley, N. E. Smith, W. H. Bernskoetter, N. Hazari and B. Q. Mercado, *Organometallics* 2018, **37**, 21, 3846-3853.
- ¹⁴ a) H. Dai, W. Li, J. A. Krause and H. Guan, *Inorg. Chem.* 2021, **60**, 6521-6535; b) Part of the results in reference 14a are very close to those described in our preprint: D. H. Nguyen, D. Merel, N. Merle, X. Trivelli, F. Capet, R. M. Gauvin, *ChemRxiv*, 2020, doi:10.26434/chemrxiv.12411020.v2.
- ¹⁵ a) A. Naik, T. Maji and O. Reiser, *Chem. Commun.*, 2010, **46**, 4475-4477; b) R. Bigler and A. Mezzetti, *Org. Lett.* 2014, **16**, 6460-6463; c) R. Bigler, R. Huber and A. Mezzetti, *Angew. Chem. Int. Ed.* **2015**, *54*, 1-5.

-
- 16 a) V. P. Boyarskiy, N. A. Bokach, K. V. Luzyanin and V. Y. Kukushkin, *Chem. Rev.* 2015, **115**, 2698–2779; b) K. T. Mahmudov, V. Y. Kukushkin, A. V. Gurbanov, M. A. Kinzhalov, V. P. Boyarskiy, M. F. C. Guedes da Silva and A. J. L. Pombeiro, *Coord. Chem. Rev.* 2019, **384**, 65–89; c) M. Knorn, E. Lutsker and O. Reise, *Chem. Soc. Rev.*, 2020, **49**, 7730–7752.
- ¹⁷ a) L. Zhang, G. Raffa, D. H. Nguyen, Y. Swesi, L. Corbel-Demailly, F. Capet, X. Trivelli, S. Desset, S. Paul, F. Paul, P. Fongarland, F. Dumeignil and R. M. Gauvin, *J. Catal.*, 2016, **340**, 331–343; b) D. H. Nguyen, G. Raffa, Y. Morin, S. Desset, F. Capet, V. Nardello-Rataj, F. Dumeignil and R. M. Gauvin, *Green Chem.* 2017, **19**, 5665–5673; c) D. H. Nguyen, X. Trivelli, F. Capet, J.-F. Paul, F. Dumeignil and R. M. Gauvin, *ACS Catal.* 2017, **7**, 2022–2032; d) D. H. Nguyen, X. Trivelli, F. Capet, Y. Swesi, A. Favre-Réguillon, L. Vanoye, F. Dumeignil and R. M. Gauvin, *ACS Catal.* 2018, **8**, 4719–4734.
- ¹⁸ M. Käß, A. Friedrich, M. Drees and S. Schneider, *Angew. Chem. Int. Ed.* 2009, **48**, 905–907.
- ¹⁹ A. Friedrich, M. Drees, M. Käss, E. Herdtweck and S. Schneider, *Inorg. Chem.* 2010, **49**, 5482–5494.
- ²⁰ C. Bianchini, D. Masi, A. Romerosa, F.; Zanobini and M. Peruzzini, *Organometallics* 1999, **18**, 2376–2386.
- ²¹ M. S. Rahman, P. D. Prince, J. W. Steed and K. K. Hii *Organometallics* 2002, **21**, 4927–4933.
- ²² S. S. Rozenel and J. Arnold, *Inorg. Chem.* 2012, **51**, 9730–9739.
- ²³ a) R. W. Stephany, M. J. A. de Bie and W. A. Drenth *Org. Magn. Reson.* 1974, **6**, 45–47; b) P. Cmoch, R. Głaszczka, J. Jaźwiński, B. Kamieńska and E. Senkara, *Magn. Reson. Chem.* 2014, **52**, 61–68; c) P. Cmoch and J. Jaźwiński, *J. Mol. Struct.* 2009, **919**, 348–355.
- ²⁴ K. Matsubara, S. Mima, T. Oda and H. Nagashima, *J. Organomet. Chem.* 2002, **650**, 96–107.
- ²⁵ A. Friedrich, M. Drees, J. Schmedt auf der Günne and S. Schneider, *J. Am. Chem. Soc.* 2009, **131**, 17552–17553.
- ²⁶ Analysis of crystals by ¹H and ¹¹B NMR shows the presence of BEt₄⁻: ¹H NMR (285K, C₇D₈, 400.33MHz, ppm): δ ; ¹¹B{¹H} NMR (285K, C₇D₈, 128.4418 MHz, ppm): δ -16.14 (s, 1B). The formation of [BEt₄]⁻ probably comes from the disproportionation reactions of NaHEt₃ or the commercial [Na(HBEt₃)] may contain significant quantities of [BEt₄]⁻. See refs: a) G. Smith and D. J. Cole-Hamilton, *J. Chem. Soc., Chem. Commun.* 1982, 490–491. b) G. Smith and D. J. Cole-Hamilton, *J. Chem. Soc. Dalton Trans.* 1983, 2501–2507.

-
- ²⁷ G. A. Jeffrey and W. Saenger, *Hydrogen Bonding in Biological Structures*; Springer: Berlin, **1991**.
- ²⁸ N. P. N. Wellala, J. D. Luebking, J. A. Krause and H. Guan, *ACS Omega* 2018, **3**, 4986.
- ²⁹ S. Kar, R. Sen, J. Kothandaraman, A. Goepfert, R. Chowdhury, S. B. Munoz, R. Haiges and R. G. S. Prakash, *J. Am. Chem. Soc.* 2019, **141**, 3160–3170.
- ³⁰ G. A. Filonenko, R. van Putten, E. J. M. Hensen and E. A. Pidko, *Chem. Soc. Rev.* 2018, **47**, 1459–1483.
- ³¹ The anion exchange reaction from the *cis-8* and *trans-8* mixture affords the related complexes *cis-9* and *trans-9*, from which *cis-9* can be obtained as pure compound from crystallization. Only *cis-9*-related data is reported here.
- ³² a) S. M. Tetrick and R. A. Walton, *Inorg. Chem.* 1985, **24**, 3363–3366; b) W. D. Jones and W. P. Kosar, *Organometallics* 1986, **5**, 1823–1829.
- ³³ R. A. Michelin, A. J. L. Pombeiro and M. F. C. Guedes da Silva, *Coord. Chem. Rev.*, 2001, **218**, 75–112.
- ³⁴ L. De Luca, A. Passera and A. Mezzetti, *J. Am. Chem. Soc.* 2019, **141**, 2545–2556.
- ³⁵ A. Naik, T. Maji and O. Reiser, *Chem. Commun.* 2010, **46**, 4475–4477.
- ³⁶ S. B. Duckett, J. P. Lowe and R. J. Mawby, *Dalton Trans.* 2006, 2661–2670.
- ³⁷ W. Ma, S. Cui, H. Sun, W. Tang, D. Xue, C. Li, J. Fan, J. Xiao and C. Wang, *Chem. Eur. J.* 2018, **24**, 13118–13123.
- ³⁸ G. M. Sheldrick, SHELXT – Integrated space-group and crystal-structure determination. *Acta Crystallogr. Sect. A* 2015, **71**, 3–8.
- ³⁹ G. M. Sheldrick, Crystal structure refinement with SHELXL. *Acta Crystallogr Sect. C* 2015, **71**, 3–8.
- ⁴⁰ L. J. Farrugia, ORTEP-3 for Windows - a version of ORTEP-III with a Graphical User Interface (GUI); *J. Appl. Crystallogr.* 1997, **30**, 565.